

Chapter 1

Getting Started : Some Basics

1.1 Introduction

The demand for energy has grown speedily in current years, with the expansion of industry and economy. In the last century, fossil fuels, such as coal and oil, have been promoting industrial development. Though, extreme fossil fuel consumption has made mankind face rising pressure from energy insufficiency and environmental issues, such as global warming and acid rain. The energy crisis has turned into a global challenge. The need for alternative energy sources which are environmentally friendly is more acute than ever[13].

Wind power, due to its extensive distribution across the globe, is one of the most common basics of renewable energy. A wind turbine can produce electricity by converting the kinetic energy from wind into electric and mechanical energy[13,15]. Unlike fossil fuels, it produces very little to no greenhouse gas at all, and thus can help ease global warming efforts. Since wind energy is becoming progressively popular, improving the efficiency of wind turbines is of importance, leading to increased research in this field.

Two wind turbine types exist: Horizontal Axis Wind Turbine (HAWT) and Vertical Axis Wind Turbine (VAWT). Because of its higher aerodynamic power coefficient, the former is more common compared to the latter. VAWTs however offer certain special advantages that HAWTs do not have. VAWT's power output is independent of the flow's inbound course. Additionally, VAWTs can be mounted at a wide

variety of wind speeds, creating lower noise. They have mechanical systems relatively simpler, and are easier to manage than HAWTs.

The efficiency of wind turbines is essentially determined by the shape of the blade. The aerofoils are the blade's foundational element. They have a tremendous influence on turbine aerodynamic performance. Nowadays, there are several methods available to boost wind turbine aerodynamics and resolve the disadvantages, such as optimizing blade form [1, 2], incorporating intelligent control system and enhancing generator design. One of the commonly used techniques of raising the rotor's power coefficient is flow control of wind turbine blades, among them.

This project deals with Performance evaluation and optimisation of Lift type Vertical Axis Wind turbines. This has been carried out using a Computational Approach, in which the commercial CFD software Ansys Fluent has been used. This report has been structured into 5 chapters, the first presents an introduction of Vertical Axis wind turbines (VAWTs), their configurations and various other parameters pertaining to their performance. The chapter also includes a comparative study of VAWTs and HAWTs, which aims to inform the reader about the advantages of VAWTs and the potential they hold. The second chapter, deals with the optimisation of parameters using meta-heuristic algorithms, such as the one used in this study (the genetic algorithm). This chapter aims to introduce the reader to such algorithms and form a foundation which can be expanded in the subsequent chapters as the optimisation of Aerofoil Profile is elaborated.

The third chapter dwells upon the actual optimisation algorithm used in this project to obtain a high performance airfoil section. This section also talks about the limitations of the approach used and the steps taken to overcome them. It will further elaborate on the use and advantages of multi-step optimisation algorithm such as the one used here, as opposed to single-step optimisation algorithms.

The fourth chapter deals with VAWTs. Here the optimised airfoil section is implemented into VAWTs and the resulting performance parameters are compared to the commonly used airfoil sections. The specifics including the fine-tuning of computational fluid dynamic models are discussed, the help in a more reliable and faster convergence. Furthermore, certain numerical algorithms that are used to calculate the time-integrated/ time-averaged quantities are discussed.

The Fifth and Final chapter deals with the future scope and improvement opportunities of this project. It

also Elaborates on the use of alternative algorithms for optimisation of aerofoil sections. Furthermore, this chapter involved the discussion on techniques other than algorithmic optimisation, that can be used to improve the performance of VAWTs.

1.2 Literature Survey

In the study conducted by Junkun Ma et al., Pitch and Camber control are emphasized, It has been established that such practices help in improving VAWT performance, The aim of this study is to study the pressure field on the airfoil surface and to develop an optimal airfoil pitch control strategy to extract maximum power output from the VAWT. It has been noted that, Wind velocity has a lower effect on both, the magnitude of torque and its distribution as compared to airfoil AoA. It was found that for NACA 0012 airfoil, torque peaks at 9 degree AoA irrespective of the support arm position. Changping Liang and Huaxing Li[10] have used the XFOIL program (for pre-stall performance), in tandem with ViternaCorrigan post-stall model for optimisation. The study was computational in nature, and the ANSYS Fluent commercial package was used. The airfoil used was NACA 0015, and an increase in the power performance was sought. Class and shape function transformation parametrization method was used to produce changes in the airfoil profile. The parameters in the genetic algorithm were the airfoil thickness and camber, much like in the present study. The objective function chosen was the maximum tangential force coefficient. It was seen that, the optimized aerofoils lift to drag ratio was improved over a wide range of attack angles and the stall performance was gentler. The maximum lift coefficient, the maximum lift to drag ratio and the maximum tangential force coefficient were improved significantly. In the study conducted by B. Allen Gardner and Michael S. Selig[6], optimal airfoil shapes were constructed through manipulation of the velocity distribution by a genetic algorithm, this is an inverse method as it tries to construct an optimal airfoil profile from a desired velocity distribution profile. A viscous-flow analysis code, much like Xfoil and Profoil was used to determine thickness values for airfoils. A comparison was carried out between direct and inverse approaches, based on their use in the optimisation process. Later, the inverse approach was coupled to a simple genetic algorithm and a hybrid algorithm and the resulting airfoils were compared. The hybrid algorithm combined a local search provision in the already existing code (SGA plus Inverse method). Results indicate that using the design variables defining the velocity distribution in the inverse method possesses tremendous potential for improving the performance of heuristics based airfoil shape optimization algorithms. In the study conducted by Shoutu Li et al.[9],

the objective was to maximize the aerodynamic performance of the airfoil by optimizing its geometrical parameters, a new airfoil was found which was called the LUT (Lanzhou University of Technology) airfoil, by employing the sequential quadratic programming, much like the fmincon optimisation methon in MATLAB. The LUT airfoil, with a wide drag bucket and gentle stall performance, achieves a higher maximum lift coefcient and liftdrag ratios in the Reynolds numbers range of 310^5 and 510^5 . In Sayyad Basim Qamara and Isam Janajreha's work[15], Cambered blades were investigated using high fidelity CFD modelling under unsteady, turbulent regimes using arbitrary Eulerian and Lagrangian approaches with sliding mesh configuration to gain more knowledge of their interactions and the effect on turbine performance. This work pretty much covers the basics of VAWT simulations. The objective was, assessing the performance of Cambered airfoils in VAWTs and comparing them to the more conventionally used, symmetrical airfoils. This work primarily took into consideration, the Coefficient of Performance, the tip speed ratio and the torque produced by the airfoils. It was seen that airfoils with camber can produce a significantly higher coefficient of performance than conventional airfoils. However, it was hinted that perhaps, too high a camber could be detrimental to the VAWT performance. Furthermore, it was found that cambered airfoils are better suited for low wind speed applications, from this study's scope, during low TSR regimes of operation. As is quite trivial, airfoils with a moderate camber also improved the self starting capability of the VAWTs. In the work done by Krishna Vijayaraghavan et al.[8], an important consideration made is the choice of maximising the C_t value as opposed to C_l value, such a consideration is made because, the coefficient of tangential force is a much more suited indicator of the power performance of the VAWT. This paper attempts to study the effects of profile perturbations on a NACA 0015 Airfoil. It is important to point out that the perturbations made, involved the addition of supplementary lift-drag characteristic improving devices, like Gurney flaps and inward dimples. Parameters like the dimple radius and the height of the gurney flap were optimised. It was seen that the optimised airfoil had a better tangential force (higher) than the baseline NACA 0015. In the wrk done by Ryan McGowan, Rafael Lozano, and Vrishank Raghav[21], the aim was to overcome the self-starting issues associated with VAWTs and abate problems pertaining to low tip speed ratio operations. Various factor were examined, such as increasing the solidity to reduce blade interference, guide vanes to direct flow were considered. Performance of turbines was calculated and trends were compared to the data obtained from the literature. This work also examined the properties pertaining the drive systems for the VAWTs. The simulation program was adapted from various sources and consolidated to produce better and more reliable results. The nature of the work were both Analytical and computational. In Drew

A. Curriston Alice E. Smith's[23] study, evolutionary algorithm along with Bezier Curves are used to generate optimal Airfoil, the Airfoil requirement is not restricted to VAWTs and Bezier curves are not restricted, movement in both x and y direction is allowed. Addresses subsonic airfoil optimisation using evolutionary algorithms The Evolutionary Algorithms allowed for a continuous manipulation process in the shape of the airfoil when coupled with Bezier curves to produce the shape. It was found that airfoils were optimised extremely well. This method was proposed for a wide range of airfoil profile optimisations. In Ayat Forouzandeh et al.[7]'s work, the performance of NACA 0018 and DUW 200 airfoils were compared. The comparison was carried out by varying the solidity, number of blades and TSR. Additional parameters like the turbine aspect ratio were also explored in detail and the results were quoted. It was found that the favourable range of solidity was between 0.3 and 0.5, and above this range it was seen that the power coefficient decreases significantly. Regarding the number of blades, it was observed that a 3 bladed configuration was favourable and performed better than any 4 or 2 bladed configuration.

1.3 Mathematical Models

The governing equations for external flow field are the compressible or incompressible Navier-Stokes equations (Compressibility dependent on the flow conditions like density, Mach number and Temperature). These equations have been solved using an implicit solver for all simulations. The governing conservation equations for mass, momentum, and energy are[5],

$$\frac{\partial \rho}{\partial t} + \nabla \cdot (\rho V) = 0 \quad (1.1)$$

$$\frac{\partial \rho V}{\partial t} + \nabla \cdot (\rho V V) = -\nabla \cdot (p) + \nabla \cdot (\tau) \quad (1.2)$$

$$\frac{\partial \rho E}{\partial t} + \nabla \cdot (V(\rho E + p)) = -\nabla \cdot (k \cdot \nabla(T) + \tau \cdot V) \quad (1.3)$$

$$E = h - \frac{p}{\rho} + \frac{V^2}{2} \quad (1.4)$$

$$\tau = \mu \left((\nabla V - \nabla V^T) - \frac{2}{3} \nabla \cdot V I \right) \quad (1.5)$$

The above system of equations is closed by the Ideal Gas Equation in compressible flow studies. In these equations, E is the specific energy, and p is the absolute local pressure, μ is the fluid viscosity, k is the thermal conductivity, T is the static temperature, h is the enthalpy, and τ is the viscous stress tensor. From the above equations, the energy equation is omitted and density kept constant in case of incompressible flow conditions. A pressure based solver has been used for all incompressible simulations. The solver makes use of the coupled pressure-velocity coupling. The turbulence model used is the $K - \omega SST$ two equation model. In case of low Reynolds numbers, the intermittency model was also used with $K - \omega SST$ making it a three equation model[17].

Kinematic Eddy Viscosity

$$\nu_T = \frac{a_1 K}{\max(a_1 \omega, SF_2)} \quad (1.6)$$

Turbulent Kinetic Energy

$$\frac{\partial Q}{\partial t} + U_j \frac{\partial k}{\partial x_j} = P_k - \beta * k * \omega + \frac{\partial}{\partial x_j} \left[(\nu + \sigma_k \nu_T) \frac{\partial k}{\partial x_j} \right] \quad (1.7)$$

Specific Dissipation Rate

$$\frac{\partial \omega}{\partial t} + U_j \frac{\partial \omega}{\partial x_j} = \alpha S^2 - \beta_P \omega^2 + \frac{\partial}{\partial x_j} \left[(\nu + \sigma_\omega \nu_T) \frac{\partial \omega}{\partial x_j} \right] + 2(1 - F_1) \sigma_\omega \frac{1}{\omega} \frac{\partial k}{\partial x_i} \frac{\partial \omega}{\partial x_i} \quad (1.8)$$

These equations represent the mathematical equations used in the turbulence model. It can be seen that there are two important transport equations, one for turbulence kinetic energy and the other for specific dissipation rate. These equations are only included as additional information to the reader. Further information regarding the specifics of turbulent transport equations is out of the scope of this report.

Chapter 2

A Discussion on Vertical Axis Wind Turbines

2.1 Vertical Axis Wind Turbines

A vertical axis wind turbine is a wind turbine in which the main rotor shaft is set transverse to the wind. In this type of wind turbines the generator is set at the base. This is seen as an advantage of these wind turbines over horizontal axis wind turbines in which the generator is placed as a considerable height above the ground. The placement of the generator and other parts like the gearbox at the base (i.e. at the ground level) facilitates repair and maintenance[25]. Furthermore VAWTs are designed in such a manner that they are always facing in the wind, this means that they do not require any yawing mechanisms or any wind sensing mechanisms[3]. The use of VAWTs is however, only limited to small scale applications. The use of such wind turbines in large setting s is generally avoided, because of lower performance[5]. For instance, such wind turbines show a periodic variation in the torque produced. This is because at any given time, only some of the blades are producing useful power while the others are either idle or are drag producing. There have been improvisations that were aimed at reducing this ripple effect in VAWTs. One of the most commonly known improvisation is sweeping the blades in a helical orientation[9].

2.2 Types of Vertical Axis Wind Turbines

Broadly classifying, VAWTs may be comfortably classified as Lift based and Drag Based wind turbines. This classification is associated with the production of the force that produces power. That means, it takes root in the method of power production[10].

2.2.1 Lift Type Wind Turbines

In Lift type wind turbines the Lift force is the primary torque producing force. The geometry of a Lift type wind turbine includes blades with airfoil section, pointed into the rotary direction of the VAWT. It is by virtue of the lift force, that torque is generated. The induced angle of attack of the Lift type VAWTs is the inclination of vector resultant of the angular velocity and the freestream velocity[25]. The parameter that measures the relative magnitudes of the freestream velocity and the angular velocity is the tip-speed ratio, which shall be discussed later in detail[7].

2.2.2 Drag Type Wind Turbines

Drag type wind turbines are perhaps the simplest wind turbines available and have been existing for a very long time. The power producing force here is the drag force, which is generated when air-stream hits the vanes of the wind turbine. Notice how drag type wind turbines contain vanes as compared to blades in Lift type wind turbines. These wind turbines rotate in the direction of the free stream flow (the wind pushes the vanes)[25]. Although the design of drag type wind turbines is very simple, the performance is generally poor. These wind turbines do not find a lot of industrial application.

2.3 Aerodynamics of Vertical Axis Wind Turbines

This section deals with the aerodynamics of Vertical Axis Wind turbines. The aerodynamics of the different types of wind turbines is similar in that the induced angle of attack is the same in both Lift based and Drag based VAWTs[17]. The induced angle of attack however, does not have much application in drag type VAWTs. We shall consider the general aerodynamics in a bite-sized and a stepwise procedure here. Consider the Resultant velocity \vec{W} of the Wind turbine. It can be mathematically written as the vector sum of the free stream velocity (V_∞) and the velocity vector of the blade advancing, $-\omega x R$, That means,

$$\vec{W} = \vec{V}_\infty + (-\vec{\omega} \times \vec{R}) \quad (2.1)$$

This means that the fluid velocity varies in every rotation of the wind turbine, and is a function of the angle of rotation θ . Consider figure 1. It is evident that the resultant velocity is maximum at $\theta = 0^\circ, 180^\circ$ [15,23,24]. Particularly for a Lift type VAWT, the discussion of the induced or the oncoming angle of

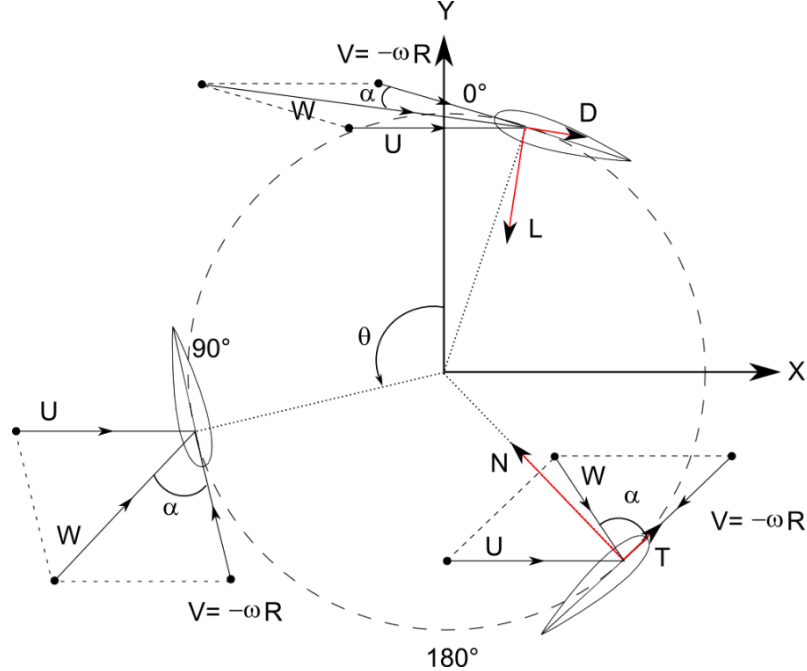


Figure 2.1: Aerodynamics of Vertical Axis Wind Turbines

attack is of extreme importance, as it directly influences the performance of the VAWT[11]. For this reason the following equations are pivotal in the design considerations pertaining to VAWTs. Consider the tangential component of the oncoming wind vector \vec{W}

$$V_t = R\omega + V_\infty \cos\theta \quad (2.2)$$

And the normal component of the oncoming wind vector is,

$$V_n = V_\infty \sin\theta \quad (2.3)$$

For Lift type VAWTs, the tangential component of the velocity has to be maximised, which consequently maximises the tangential force produced by the blades[23,24]. An excellent measure of the performance of VAWT blades is the tangential force coefficient, given by

$$C_t = C_l \sin\theta - C_d \cos\theta \quad (2.4)$$

Generally, the c_t value is considered to be the objective function in the selection of blade profiles.

2.4 Advantages of VAWTs over HAWTs

1. VAWT needs much lower fabrication costs than an equivalent size HAWT. In the period in-between, the engine, brake and transmission system are mounted on the site, which is easy to mount, maintain and inspect.
2. A VAWT does not need a yaw system, and can therefore absorb wind energy from either direction[24].
3. A VAWT has relatively low rotational velocity and thus creates low noise.
4. A VAWT can endure high-speed wind, being able to work safely.

2.5 Configurations of Vertical Axis Wind Turbines

This section briefly discusses the different configurations in which VAWTs are found. These configurations differ essentially based on their geometry and power generation characteristics. While some lay more emphasis on ease of manufacturing and lower costs, other configurations are specifically targeted to produce more power and hence have a higher efficiency. We already saw in the previous sections how VAWTs can be classified into two types, i.e. drag-type devices and lift-type devices. Savonius VAWTs are the most typical for first type. The Savonius VAWT is a drag-type device composed of two or three scoops, aerodynamically. Looking down from above, there's an S-shaped cross section on a two-scoop unit. The scoops feel less friction when moving against the wind than they do with the wind because of the curvature. As shown in Fig. 2 the differential drag causes the Savonius turbine to spin. Since Savonius turbines are drag-type machines, such equipment harnesses significantly less wind energy than similar-scale lift-type turbines [2,4]. The most common for second form are Darrieus VAWTs. When a Darrieus rotor spins, the airfoils move in a circular direction through the air[14,16]. This approaching airflow, relative to the blade, is applied to the wind in vector, so that the resulting airflow produces a varying small positive angle (AoA) for the blade. This produces a net force pointing a certain 'line-of-action' obliquely forward, giving the shaft a positive torque, as shown in Fig. 3. Darrieus VAWTs have a higher power ratio, relative to other VAWTs. Darrieus VAWTs will therefore finally be used in the current wind field and become the image of large-scale VAWTs.

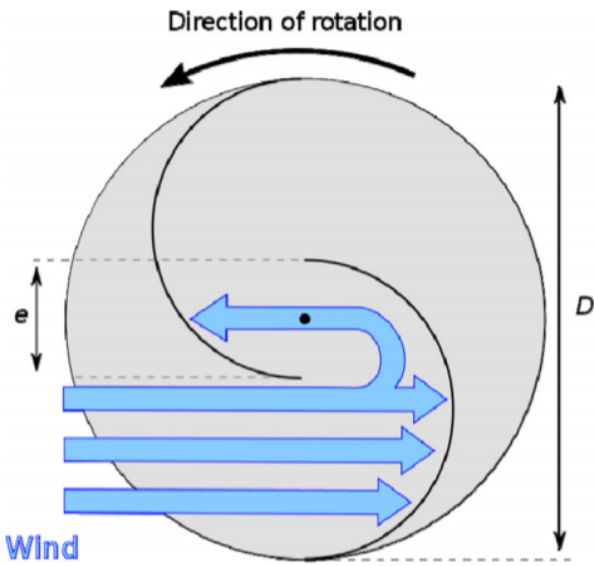


Figure 2.2: Savonius Wind Turbine (Drag type)

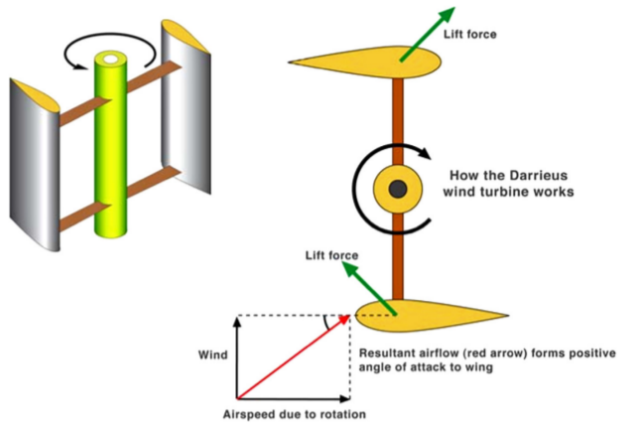


Figure 2.3: Darrieus Wind Turbine (Lift Type)

2.5.1 Some More configurations based on arrangement of blades

A. EGG-BEATER TYPE DARRIEUS WIND TURBINE

This design is characterised by curved blades, looking like an egg beater. The movement of a Darrieus wind turbine around its blades is characteristically unstable. This pulsating flow produces a thrust force that is proportionate to the blade geometry and the amplitude and frequency of the pulsating flow. The complex design of the egg-beater form implies low bending stress in the blades. Because of this increased

mechanical integrity and high performance co-efficient commercial turbines have been developed in a country as large as 3.8 MW capacities. The average value thus obtained was 0.42 at a specific TSR[24].

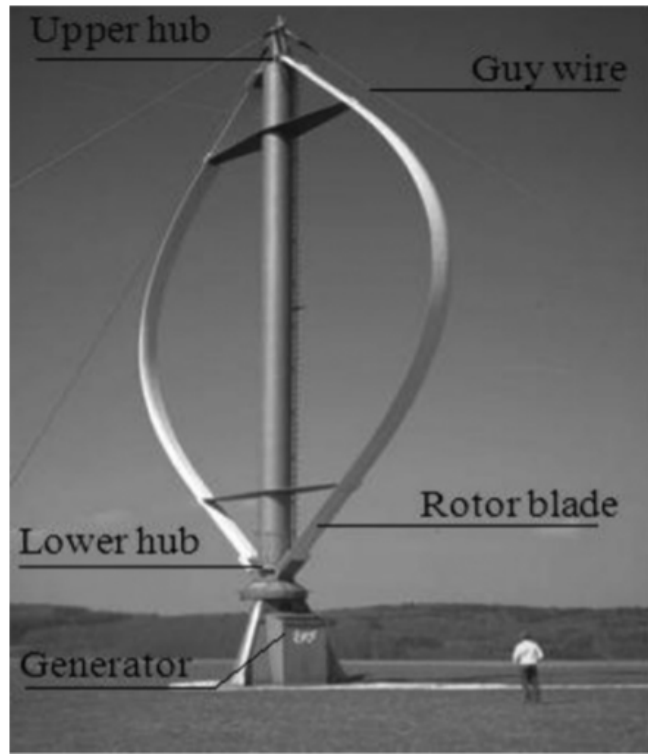


Figure 2.4: Egg-Beater Type Darrieus Wind Turbine

B. GIROMILL (STRAIGHT BLADED) TYPE DARRIEUS WIND TURBINE

In this design the curved blades used in the egg-beater configuration are substituted and instead, the blades are kept uniform and straight. The number of blades can vary from 2-5 blades, however the most commonly available are the 2 and 3 bladed configurations of this design. The advantage of this design is the ease of manufacture. This design can be manufactured very easily and the analytical/ computational analysis of this design is perhaps the easiest, considering that 2-D simulations can also be carried out. The blades used in this design can have a fixed pitch angle with the wind's angular velocity, or a variable pitch setup can also be made. Such a variable pitch setup needs additional study and actuation mechanism at every arm. This increases the complexity, but improves the performance considerably. These designs are very amiable to small scale production and are being extensively used in the domestic use market. Despite having Turbine performance has found to increase on adjusting the angle of attack in a sinusoidal

pattern on the blades[13,19,21]. Fixed pitch blades offer low starting torque although they are easy to create. Variable pitch designs have many improvements over fixed pitch, but the construction is very challenging and thus reduces the turbine's cost-effectiveness for small applications.

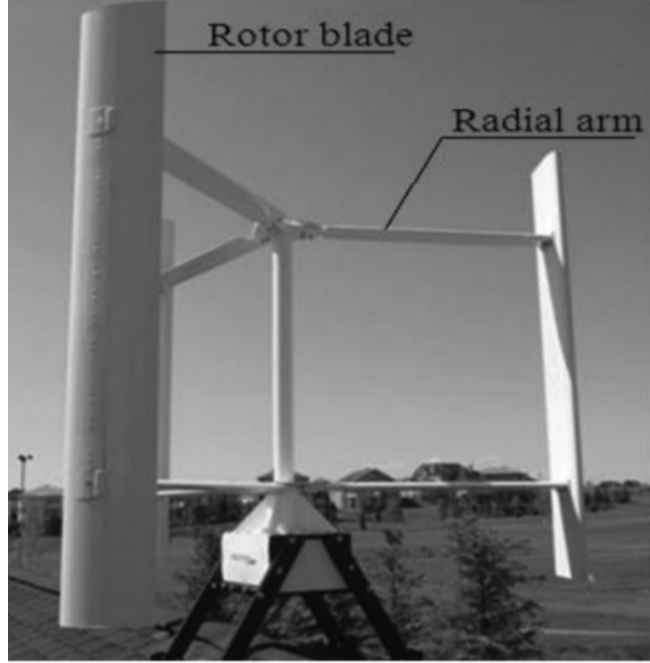


Figure 2.5: Giromill (Straight Bladed) Type
Darrieus Wind Turbine

C. VARIABLE GEOMETRY OVAL TRAJECTORY (VGOT) DARRIEUS TURBINE

Consideration of low rotor speed is a crucial characteristic of the rotor design. The designs of Darrieus turbines, cannot be used for large scale energy production. Hence a new design was developed to accommodate such features. In VGOT configuration, the mechanism is designed such that the blades travel on rails. The wheels or the bearings connected to the rotating rails are connected to generators for power production[13,24]. This design incorporates the VAWT's capability to be driven by wind from any direction, while also providing higher efficiency which is comparable to HAWTs. Furthermore this configuration also lends higher mechanical properties (better) and alleviates the starting-torque related problems. However, the design complexity does not allow for a small scale / domestic use.

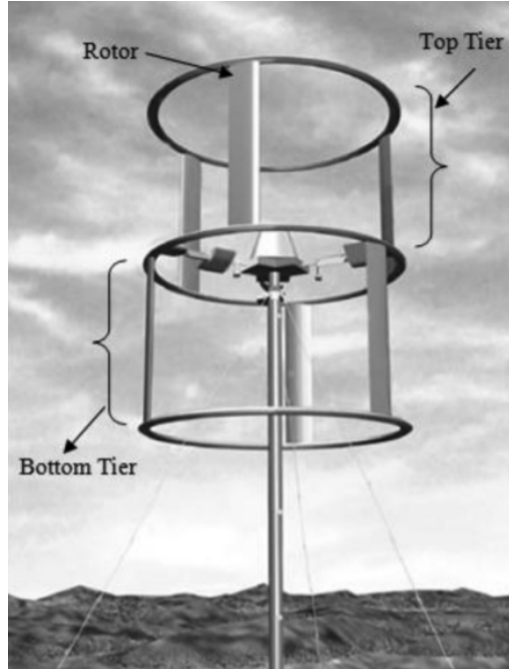


Figure 2.6: Variable Geometry Oval Trajectory (VGOT) Darrieus Turbine

E. GORLOV HELICAL TURBINE (GHT)

GHT is a turbine that was initiated from the Darrieus turbine design by making helical blades or alteration of foils. It was created by Alexander M. Gorlov, a professor in the Northeastern University. Its working principle is same as any of the Darrieus turbine family. The fundamental difference between the GHT and standard turbines is the axes' orientation toward flow. The GHT is in a perpendicular position to flow. The axis of this turbine may be either vertical or horizontal according to the water flow direction but the only restriction that flow should be orthogonal[15,16]. GHT functions under the principle of a lift. The foil pieces are symmetrical, from the leading to trailing edge. Normally, it spins in either direction equal good manner. It operates on the same principle as other Darrieus turbine does. It depends on the movement of the foils to change the outward direction of the flow relative to the foils, thereby altering the foil's (outward) "angle of attack." When building a dam is objectionable, GHT is planned for low-head micro hydro installations. It is a case of a dam less hydro technology. This could theoretically deliver price and ecological advantages compared to other micro-hydro-systems associated on dams. The twisted blades' key benefit is to diminish isolation of flow. Consequently, the resultant rotor has a positive lift

at zero angle of incidence. This allows it to start itself at advantageous wind conditions (not requiring a secondary mechanism). This results an increase in efficiency and also hence increase area of the blade projection[3,15,24]. .



Figure 2.7: Gorlov Helical Turbine (GHT)

Chapter 3

Mathematical Optimisation and Meta Heuristics

3.1 Introduction

In this chapter, a brief discussion of the subject of mathematical optimisation will be made. We shall discuss the possible types of Objective functions and the optimisation strategies, that can be used to obtain global or local optima. We shall then discuss in considerable detail, the process of optimisation employed in this project, its motivation and some of its features. A discussion shall then be made keeping in mind the future improvements possible in the algorithms used here and the possible drawbacks in the process of optimisation used here.

3.2 Definition of Difficult when it comes to Optimisation

The purpose of any optimisation process is to find the optimum values for any given parameters[26]. This value can be local if the domain of the algorithm is highly constrained or it may be the global value if the constraint is broad or covers a wider expanse. The definition of the optimum value really depends on the specific optimisation problem in question, that means, one may either want to maximise or minimise a parameter. Based on this the optima may be a local/global maxima or a local/global minima[26]. But before any step towards optimisation is taken, it is necessary to understand the features of the objective function when plotted in space. The contour or the curve that the objective function or the parameter forms is the basis for any optimisation. If the curve is functionally dependent, that means it follows a particular function, the process of optimisation becomes extremely simple. However is the curve is dis-

continuous and does not follow any given function, that means, it is random in the scope of its domain. Such functions are extremely difficult to optimise for a global optima. Consider the following figure for a better understanding of this[26]. The above function is perhaps the easiest to optimise, it is convex

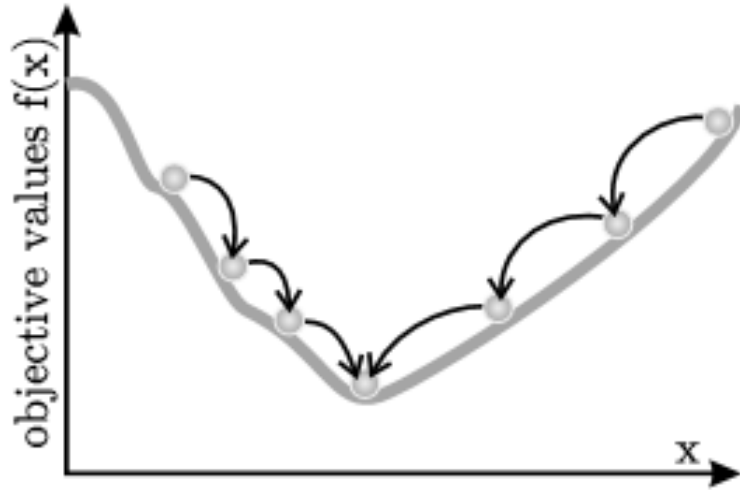


Figure 3.1: 2-D Illustration of uni-variate Convex Function[26]

function, which has a clear global minima. Here it is important to define what we really mean by a convex function.

3.3 Convex Function

In the most formal words, a convex function, is a function that satisfies the following : Let there be a convex set in a vector space and let $f : X \rightarrow R$ be a function[26]. this function is called convex if:

$$\forall x_1, x_2 \in X, \forall t \in [0, 1] : f(t.x_1 + (1 - t)x_2) \leq t.f(x_1) + (1 - t).f(x_2)$$

and would be strictly convex if :

$$\forall x_1 \neq x_2 \in X, \forall t \in (0, 1) : f(t.x_1 + (1 - t)x_2) < t.f(x_1) + (1 - t).f(x_2)$$

A function $f(x)$ is said to be (strictly) convex if $-f(x)$ is (strictly) concave. Figure 5 shows a bivariate

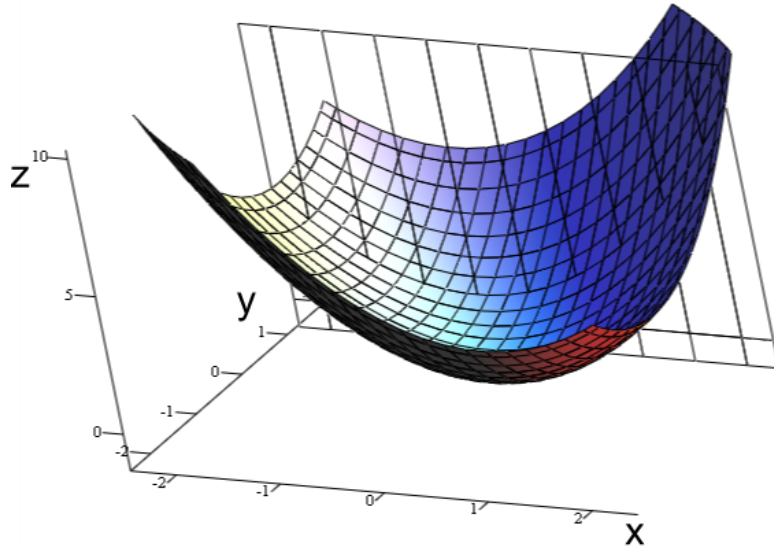


Figure 3.2: 3-D Illustration of bi-variate Convex Function[26]

convex function. Having established the formal definition of a convex function, it is quite clear why such functions are the easiest to optimise. The calculation of a minima is a simple process. Note that our discussion is only limited to a minima, because as the definition of a convex function implies, if the path of minimisation of a function is $f(x)$ then, to maximize the function one needs to solve for $-f(x)$.

3.4 Existence of Difficult Functions

While we would like to have only convex or concave functions for optimization, this isn't always the case. On multiple occasions one encounters functions that are piecewise-continuous, discontinuous or even have mathematical singularities, in the process of optimization. This is primarily the reason why optimization can be a difficult task.

3.5 Choice of Domain for Optimisation

In an optimisation process the domain is the universal set which contains all the possible solutions or configurations of the objective function. It then implies that the solution of the optimisation function is local or global , depending on the domain in which one wants to carry out the optimisation. So carry out the optimisation on a very large domain, right? Well yes, but no. If you select an extremely large domain for optimisation, your optimisation function takes that much longer to arrive at an optima, furthermore,

it the specific parameters for the optimisation are not properly set, you may never arrive at it, while this is also a problem in a smaller domain, its effects are profound in larger domains. Furthermore, on many occasions, one has constraints on the optimisation function. This is very true of functions that describe physical systems. For example. While the mathematical function describing energy of a system can very well take a negative value (mathematically!), energy can most certainly not be negative in physical systems (at least not in those pertaining to engineering). It therefore follows that one must be judicial while setting constraints for an optimisation process. While there are plenty more considerations to make in an optimisation process, considering the purpose and scope of this report, they are not included.

3.6 Multi Objective Optimisation and Pareto Optimality

One often encounters in many physical processes, that there are more than one optimisation objectives that need to be solved for simultaneously. These may also be bound to constraints. This makes the optimisation process more difficult and resource demanding[26]. A Multi-Objective optimisation can be mathematically defined as:

Finding a solution candidate x^ in X which minimizes (or alternatively maximises) the vector function*

$$f(x^*) = f_i(x^*), f_i(x^*), \dots, f_i(x^*)^T$$

and is feasible, that means, it satisfies all the constraints that it is subject to. The constraints supplied can be both inequality constraints and equality constraints.[26]

Meta Heuristics can be applied to such problems as well, however, due to the increased complexity of such problems, some definitions pertaining to the notions of a solution being optimal or better than other solutions need to be redefined. For this purpose Pareto Dominance is an important concept here.

3.6.1 Pareto Dominance

Pareto Dominance : In the context of Multi-objective global Optimisation, a solution candidate x_1 is said to dominate another solution candidate x_2 , if and only if $f(x_1)$ is partially less than $f(x_2)$. Which means,

$$\forall i \in [1, \dots, k] \quad f_i(x_1) \leq f_i(x_2), \quad \exists j \in [1, \dots, k] \quad : f_j(x_1) < f_j(x_2)$$

The dominance notions allows for the selection of one solution over the other. That means dominance

allows for deeming one solution preferable to the other[26]. The notion of Pareto Optimality is also important here, Pareto optimality simply means that, A feasible point $x^* \in X$ is Pareto Optimal if and only if there is no feasible $x_b \in X$ with $x_b \leq x^*$. The solution to a Multi-Objective Problem, is the set of feasible and non-dominated solutions which is known as a Pareto Optimal set. The following figure clearly shows this.

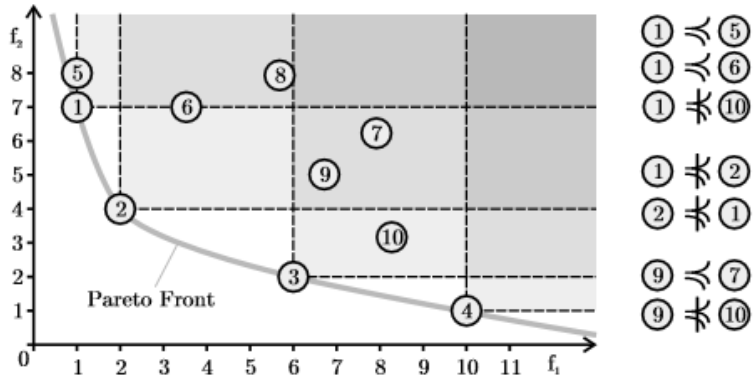


Figure 3.3: Illustration of Pareto Front in Multi Objective Optimisation

3.7 Genetic Algorithms

Genetic algorithms are widely used to generate high-quality solutions to optimization and search problems. These algorithms rely on biologically inspired operations such as mutation, crossover and selection, these algorithms fall under the broad category of Meta Heuristic Algorithms[26]. Some other algorithms that can be used in conjunction with or in the place of genetic algorithms are simulated annealing, particle swarm optimization. It is generally useful to try out direct algorithms like simplex search and, pattern search for simpler Optimisation problems. As discussed previously, the domain for the global search must be a wide yet judicial one, this ensures genetic diversity within the genetic pool of the parents and therefore ensure the genetic diversity of the subsequent generation of children. Traditionally there are three important operators of genetic algorithms, namely Mutation, Cross-over and Selection[26]. Although these are the principal operators, it is possible to use other operators such as regrouping, colonization-extinction, or migration in genetic algorithms. In a genetic algorithm, a population of offspring (called individuals, or just offspring) which are the solutions of the previous generations are evolved toward better solutions. The final solution obtained heavily relies on the crossover and mutation characteristics and

probabilities[26]. Genetic algorithms are difficult to use for simple problems because of the complexity of tuning and the time required to drive the solution toward optima.

3.8 The Operators of Genetic Algorithms

1. **Crossover :** The crossover operation, also called recombination, is a genetic operator that combines the genetic information of two parents resulting in an offspring. Different algorithms implement the crossover differently, for instance, some algorithms prefer that the offspring resulting from a crossover operation carry half of the chromosomes of both parents, In which case the crossover occurs exactly at the center of the offspring array. Some other algorithms prefer that the crossover occur randomly at any point in the array. It is important to have an additional function for checking the bounds of the resulting offspring genes. This prevent the generating of invalid solutions. Such a practice is especially important in constrained optimisation problems. Crossover operations can be single point or multi-point operations, in a single point operation, crossover occurs at a single point, whereas in a multi-point crossover occurs at multiple points, hence increasing the diversity of the generated offspring. Traditionally, the genetic information is stored in a chromosome which may be represented by a bit array/ any other array[10,26].
2. **Mutation :** The Mutation operator, essentially produces some novel changes in the genes of the parents or the offspring resulting from a crossover, to further enhance the diversity of the algorithm. In this way the genetic algorithm is able to evaluate solutions that generally would not be included in the progression of the generations, had there been no mutation. This operation should also be checked by a separate check bounds function to ensure that no invalid solutions are obtained. Furthermore, the type of mutation carried depends on the genome type: i.e. single point or multi point mutation can be employed. The mutation operation is one of the principal reasons why the genetic diversity from one generation to another is preserved. In some cases the mutation operator is made such that it adapts to the value of the objective function and goes to zero as the target value of the objective function is met. Such cases are particularly useful in local optimisation problems[10,26].
3. **Selection :** Selection is perhaps the most fundamental operator in any genetic algorithm. Selection is the process in which we select the best solutions from a population, to allow them to breed (subject them to crossover and mutation), and produce a new population (next generation). Solution

ensures that only the best individuals from a populations are allowed to , mate and the bad solutions are rejected. As with crossover and mutation, there are different types of selection processes. Some in which all the individuals in the population are considered and the best among those are selected , some in which not all the individuals are considered. The idea of keeping the best from a generation subsequent generation, is termed elitism or elitist selection. For many problems the above algorithm might be computationally demanding, for this reason, only a proportion of the individuals is considered for the next generation (truncation selection)[10,26].

Chapter 4

Airfoil Optimisation in Detail

As mentioned earlier, in this project a genetic algorithm was used to produce an optimised airfoil. The genetic algorithm was developed on python 2.7 due to the fact that python is a non-proprietary programming language. In this section the code will be explained for the benefit of the reader[26]. The pseudo code for the algorithm implementation be found in Appendix 1.

4.1 Objective Function

The objective function chosen for Optimisation was the ratio of C_l/C_d . It has been suggested in the literature to choose the tangential force coefficient for optimisation[10], however, it was found during our investigation that the tangential force coefficient can only be used as an objective function when sufficient data is provided and the camber of the airfoil is constrained. In our study, although constraints on the camber of the airfoil were imposed, they represent a much larger domain than in most of other similar studies. Furthermore, the Xfoil software was used to get the C_l and C_d data for optimisation.[26] It has been well documented that Xfoil provides a good agreement with CFD results only in pre-stall conditions, hence the data was only generated upto 15° AoA. In this range of AoA and camber constraints, it was found that C_t was not suited as an objective function.

4.2 Domain Space and Constraint Space

The search for an optimised airfoil can a wide ranged search, and the existence of a non-linear relationship between the parameters and the objective function make meta-heuristic based optimisation more difficult. It was for this purpose that a simple linear search algorithm was included in the code that narrowed down the total domain for the genetic algorithm. This was especially important because in a very wide domain, the genetic algorithm showed signs of instability and noise. The introduction of this algorithm reduced the noise and increased stability. Furthermore the time required for convergence was also decreased.[26] Figure shows a simple illustration of the concept of the domain space and the constraint space. As seen

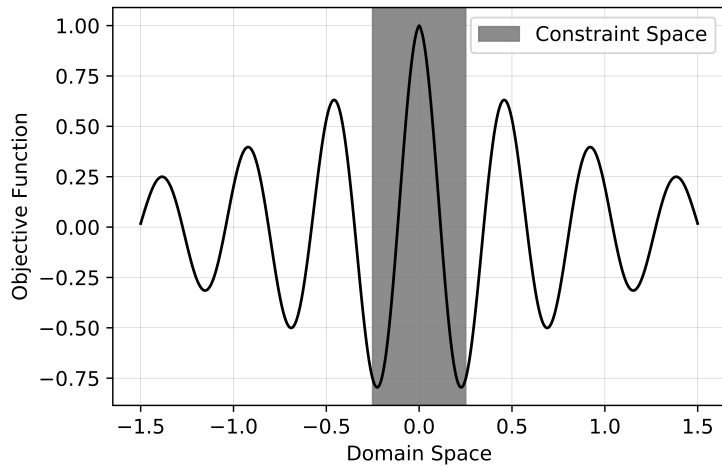


Figure 4.1: Illustration of Domain Space and Constraint Space

in the figure, the constraint space occupies a small portion of the total domain. The constraint space is found on running the linear search on regularly spaced interval in the domain set. The above illustration is a oversimplified view and the actual objective function is not so elementary[26]. After the constrained space is found, the genetic algorithm is run within the confines of this space and an optimised airfoil is produced. The produced airfoil is a local optima in this space.

4.3 Optimisation Process

This section attempts to explain the Optimisation process used to the reader in the highest degree of brevity and simplicity. The basic structure of the optimisation process, is as shown in Figure As shown

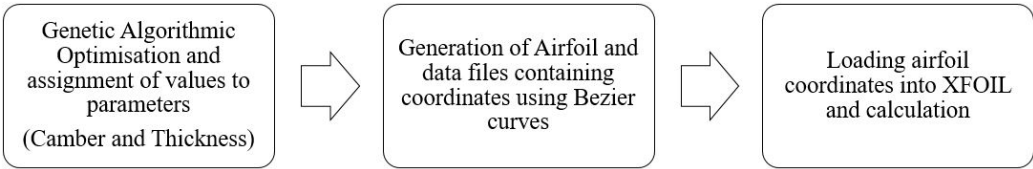


Figure 4.2: Structure of the Optimisation Process

the above flow chart, the first step of the entire process is the execution of the genetic algorithm in the constraint space. At the end of this process optimised values are assigned to parameters (camber and thickness). After this the camber and thickness details are fed to a separate code that generates the airfoil profile using Bezier curves, and saves the coordinates of the resulting airfoil in a .dat file. Finally the .dat file is imported into Xfoil where the Xfoil package calculates the Cl and Cd for the airfoil. This process is carried out for every individual in the population. The calculated Cl and Cd values are used to calculate the objective function and the genetic algorithm operates in a direction that maximises this value[26]. The Objective function is simply $\text{avg}(\text{Cl}/\text{Cd})$ for $AoA \in [0, 15]$.

4.4 Control Flow of the Genetic Algorithm

The structure of the genetic algorithm is generic, and pretty much resembles any other genetic algorithm. Figure contains a flow diagram that explains the structure and the flow of the genetic algorithm. The first step in the genetic algorithm is to set optimal constraints using the linear search algorithm, as discussed, this helps in improving the stability, reducing noise and increasing speed of the genetic algorithm. Next, random initialisation of the population is carried out. Each population contains multiple individuals (airfoils). This process is carried out at random to increase the diversity of the population. In our case a normal and uniform distribution was used. Next the fitness of each individual airfoil in the population is calculated and the best individuals are selected for breeding and producing the next generations[26]. As discussed this process is called selection. Next to introduce some diversity in the generation, the process of crossover is carried out between the selected individuals of the population. Finally the process of mutation is carried out, this introduces novel individuals in the population. It should be noted that the previous population is stored in a temporary variable. This is done so that, if the newly generated population is worse than the older one, we can get back the better population and search in a different

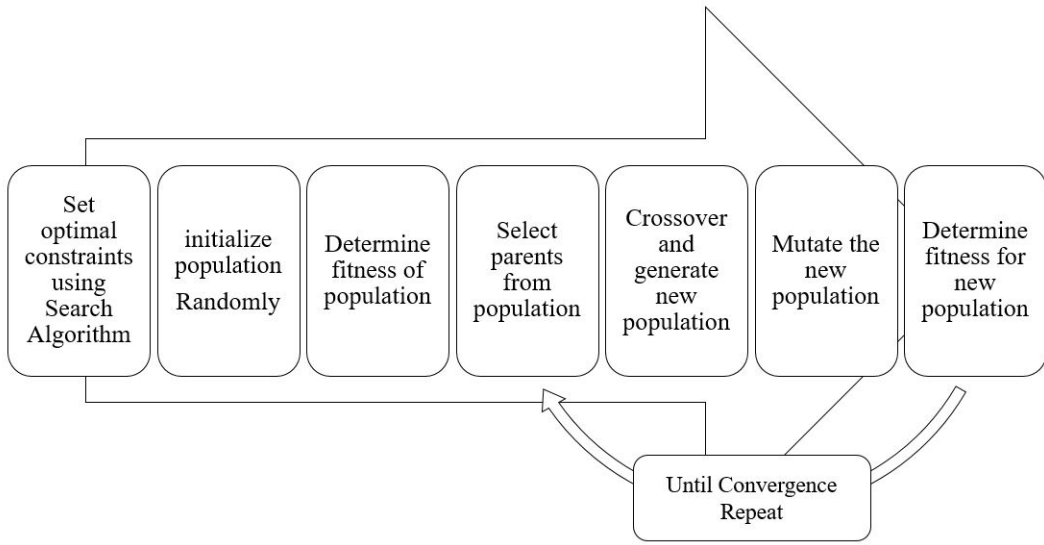


Figure 4.3: Control Flow of the Genetic Algorithm

direction. Here the elitist strategy is also important, as it makes sure that the best individuals in the previous generation are retained in the next generation. The above process is repeated until convergence (until the local optima is obtained) or until the objective function passes a certain criteria or threshold[26].

4.5 The Objective Function

The objective function is plotted against the number of airfoils, plotting the objective function against domain space and the constraint space is extremely complex, this is because of the non-linear relationship between the parameters (camber and thickness) and the coordinates of the airfoil and finally between the coordinates of the airfoil and objective function. While it is known that the camber and thickness affect the lift, the exact relationship remains obscure. Nonetheless, Figure shows the objective function as it varies with the number of airfoils tested. In the above figure, the sudden dips in the objective function depict the cases when the Xfoil program did not converge. The local maxima was found at the 77th airfoil. But another point of interest is the profile of the curve produced, it can be seen that this curve is difficult[26] (as we defined it in the previous chapter). The curve shown is neither properly concave or properly convex, hence any gradient following algorithm would have failed in finding an optima. Furthermore, this curve also points towards a possible improvement that can be made in the algorithm, that is using a better program to calculate the Lift-Drag characteristics as compared to Xfoil. Here, it is in fact possible to link this algorithm to a CFD solver, however, doing such a thing will significantly

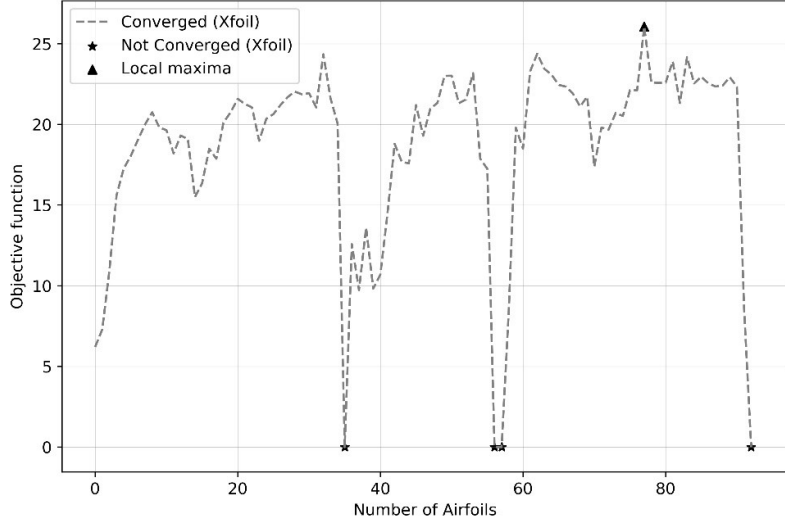


Figure 4.4: Objective Function as a function of number of airfoils

increase the time taken to reach convergence (such a method will however be more accurate). At that thought, it concludes the discussion of the profile of the objective function[26]. The pseudo code used for the optimisation will be included in Appendix 1.

4.6 Shape of the Optimised Airfoil

This section will illustrate the shape of the optimised airfoil and compare it to the baseline. Consider Figure 4.5 it shows an overlap between the shape of the optimised and baseline airfoil, so that subtle points that differentiate them can become more conspicuous. The profiles of the airfoils are magnified to allow the reader to appreciate subtle differences between the two. Clearly the optimised airfoil has a lower thickness than the baseline. This can be attributed to the fact that the airfoil optimisation process was carried out for a low Reynolds number range ($8\text{e}4$ - $3\text{e}5$). It has been documented in various studies, that as the Reynolds number decreases, the phenomenon of flow separation and formation of vortices in the wake becomes more significant. A thinner airfoil, ensures that flow separation does not occur as easily. Figure 4.6 shows the plot of the optimised airfoil alone, this will allow the reader to appreciate the camber applied by the optimisation process to the trailing edge of the airfoil. It is conspicuous that camber has been primarily applied to the trailing edge of the airfoil. The presence of camber improves the Lift performance of the airfoil, which would otherwise have been degraded due to the reduced thickness[9].

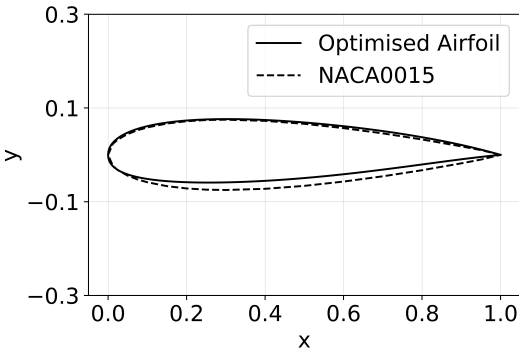


Figure 4.5: Comparison of the shape of Optimised and baseline airfoils

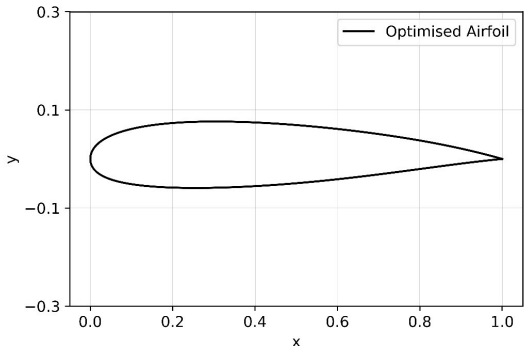


Figure 4.6: Shape of Optimised airfoil

4.7 Supplementary Material : Suitability of High Camber airfoils for VAWT Application

An additional optimisation study was conducted where, the bounds for maximum camber were relaxed. During these study the objective function used was the tangential force coefficient (C_t)[10]. The produced airfoil showed a lot of promise, in that the C_t values seen in this airfoil were the highest so far. The range of α values for which C_t was calculated was $\alpha \in [0, 15]$ (the same as for other optimisation studies)[1,5,8,26].

The importance of discussing this is that the results of this study reinforce the unsuitability of using high camber airfoils in VAWT applications. Furthermore they also point toward the unsuitability of using the tangential force coefficient as the objective function when the lift-drag data available is more a small range of α .

4.7.1 Shape of the Optimised airfoil

This section shows the shape of the optimised airfoil and compares it to the baseline. It can be seen very conspicuously from figure 4.7, that the optimised airfoil has an extreme amount of camber. This airfoil had excellent average tangential force coefficient as calculated during optimisation process. The sheer difference in the camber characteristics of the two airfoil can be discerned clearly. The Lift drag characteristic of this optimised airfoil were estimated and compared with the baseline airfoil.

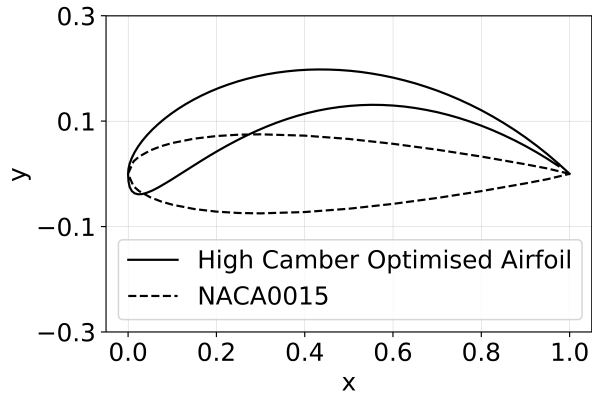


Figure 4.7: Shape of Optimised airfoil

4.7.2 Lift Drag Characteristics of High Camber Optimised Airfoil

This section presents the comparison between the lift drag characteristics of the optimised airfoil and the baseline[15]. It was found that the optimised airfoil produced significantly higher amount of lift but also has a sizable increase in the amount of drag produced. Figures 4.8-4.9 illustrate this.

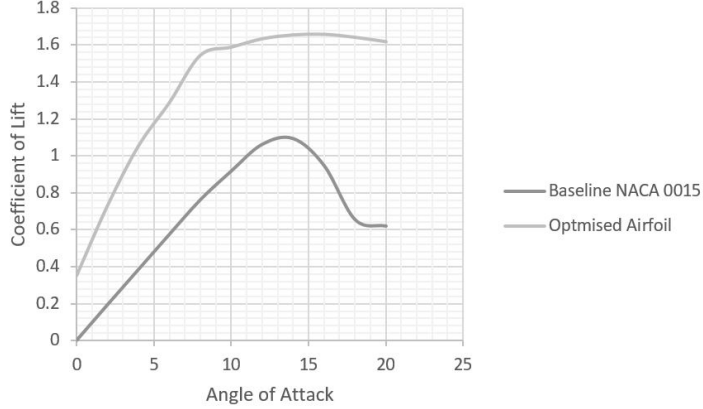


Figure 4.8: C_l VS α comparison between high camber Optimised and baseline

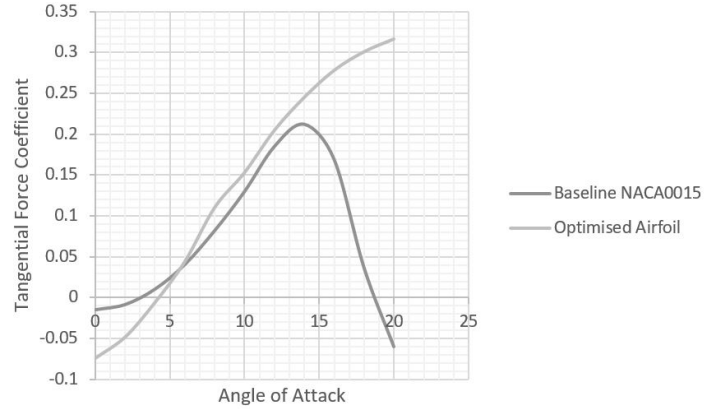


Figure 4.9: C_t VS α comparison between high camber Optimised and baseline

4.7.3 Gurney Flaps on High Camber optimised airfoil

The effect of attaching gurney flaps to high camber optimised airfoil were also studied, it was suggested in the literature that the presence of gurney flaps toward the lower trailing edge of the airfoil improved the performance of the airfoil[19,20,21,22]. The high cambered optimised airfoil already has very good

performance, however it was seen whether the use of gurney flaps could further enhance it. Figure 4.10 shows the results of the comparison of the performance of the high cambered airfoil with and without gurney flaps. Two configurations of gurney flaps were tested, one where the flaps were perpendicular to the chord line and one where the flaps were perpendicular to the camber-line[15]. From Figure 4.10, it

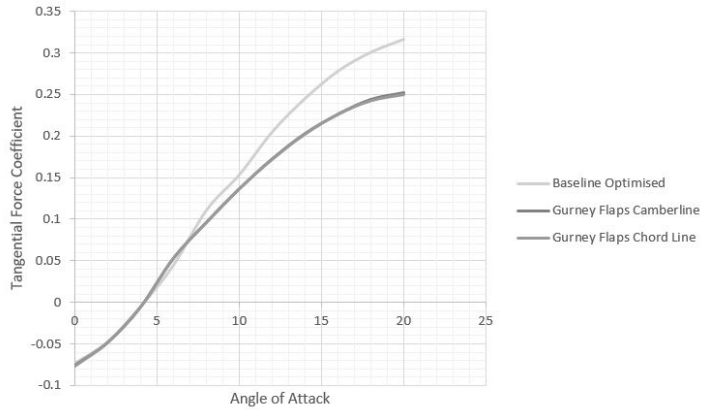


Figure 4.10: Comparison between gurney flap equipped and unequipped optimised airfoil

is quite clear that firstly, the performance of the two configurations of gurney flaps is almost identical. Secondly, It was seen that the high cambered optimised airfoil which was unequipped with gurney flaps had the best performance. This indicates that gurney flaps are perhaps not useful in high camber airfoils. Further study of this particular topic need to be conducted.

4.7.4 Unsuitability of High Cambered airfoils in VAWTs

Upon using the above airfoil in VAWT simulations, it soon became clear that high camber airfoils are inappropriate for Vertical Axis Wind Turbine applications. There are plenty of reasons for this. Firstly it was seen that for this particular airfoil, the lift-drag performance degraded rather significantly at high α . Next, and this is more generic of high cambered airfoils, that in a VAWT, the ideal airfoil is the one which can produce the same amount of performance both in the upright and upside down configuration. This is because, in a VAWT, due to the rotation, the airfoil is exposed to :

1. High range of α .
2. Is upside down for a significant portion of one rotation.

This is where a major disadvantage in high camber airfoils is exposed. Such airfoils can only produce high performance when they are upright (when they have positive camber)[9]. When these airfoils are flipped they possess a negative camber which results in major performance degradation[9].

Chapter 5

Simulations of Airfoils and VAWTs

In this chapter the CFD results of the baseline and optimised airfoil are discussed. Furthermore, the simulations of the resulting VAWT and their results are discussed. The following process for carrying out the simulations was carried out :

1. Validation with existing/published work.
2. Mesh Independence study.
3. Comparison of the baseline airfoil with optimised airfoil.
4. Comparison of the tangential force coefficient in both the cases.
5. Simulations of VAWT using baseline airfoil and plotting $C_p vs \lambda$
6. Simulations of VAWT using optimised airfoil and plotting $C_p vs \lambda$
7. Comparing the $(C_p vs \lambda)$ baseline and $(C_p vs \lambda)$ optimised.

5.1 Getting Started With Simulations

Before diving into the simulations there are some prerequisite points that need to be addressed. These points pertain to the models and the reasoning behind the use of such models. Most importantly, since VAWTs are moving/ dynamic devices, the sliding mesh methodology was implemented. For the benefit of the reader, there are two important methodologies that can be used in such systems (which have a rotary motion). These are, Moving Reference Frame (MRF) and Sliding Mesh methodology[1,2,3,4,5]. The MRF methodology is used with steady state solver, while this could have been used in our study, it

was found that the result obtained with Sliding Mesh methodology was more accurate when compared to the MRF method. It should be noted that the Sliding Mesh method is used with transient solver, and hence requires a considerable amount of computational time. Figure 5.1 shows an illustration of a sliding mesh domain.

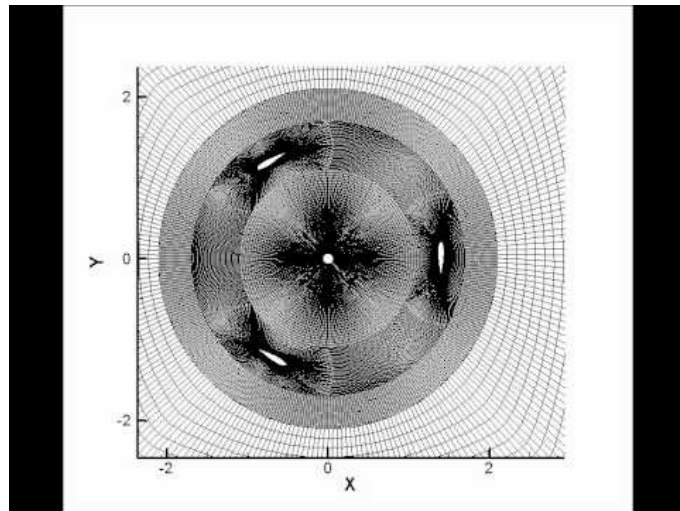


Figure 5.1: Illustration of Sliding Mesh

5.2 Choice of fluid and properties

The fluid that was used for all the simulations was Air. Table 5.1 shows the models chosen from different simulations

Table 5.1: Property Table

Property	Compressible	Incompressible
Solver	Density Based	Pressure Based
Density	Ideal gas	Constant
Specific heat(constant pressure)	Polynomial	Constant
Thermal Conductivity	Polynomial	Constant
Viscosity	3 coefficient Sutherland	Constant
Energy Equation	Enabled	Disabled

5.3 Validation Study of Baseline Airfoil

In this section the validation study conducted in order to establish a valid computational model for further simulations is discussed in detail[10]. The discussion of the said study will be done in the following parts :

5.3.1 Geometry Used

Figure 5.2 shows if the geometry used in the simulation of the Baseline airfoil. From figure it can be

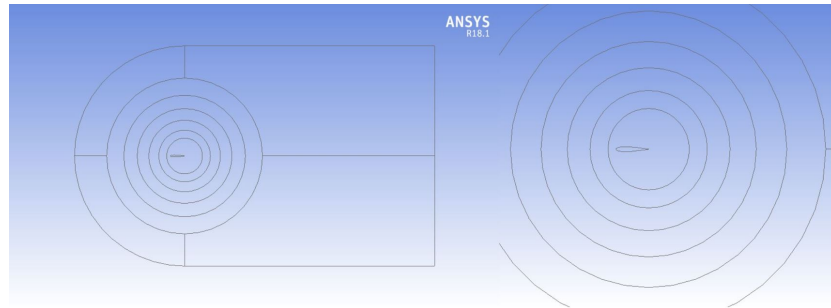


Figure 5.2: Geometry used in airfoil validation study

seen that the geometry used for simulations is blocked, for better size control. The shape of the geometry is so chosen, to allow the flow direction to be changed without requiring any changes in the geometry. Each circular block has different sizing characteristics, this allows for a gradual increase in size from the airfoil to the outer domain.

5.3.2 Meshing

Figures 5.3-5.4 show the mesh used in these simulations, the meshing methods used include, face sizing, edge sizing, inflation near the airfoil and refinement on the outer domain. From figure, it can be seen that the element size decreases gradually as one moves from the airfoil to the domain. Furthermore, inflation layers have been introduced at the airfoil, to better resolve the boundary layer formed. A gradual decrease in the element size is important to stabilise the solution and increase its accuracy.

5.3.3 Setting the Solver

The simulations were carried out using the pressure based solver, since the flow velocity involved was low and the density was more or less constant. Furthermore, thermal effects were unimportant, hence the

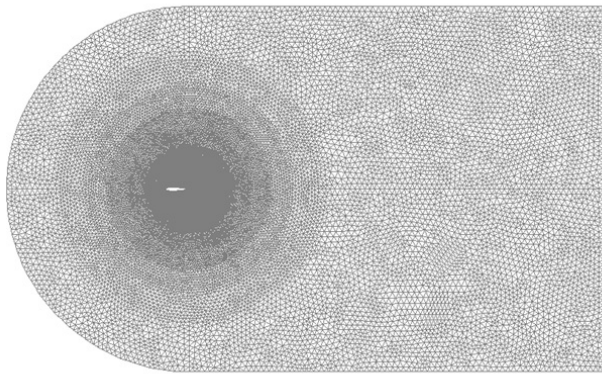


Figure 5.3: Complete View of Mesh

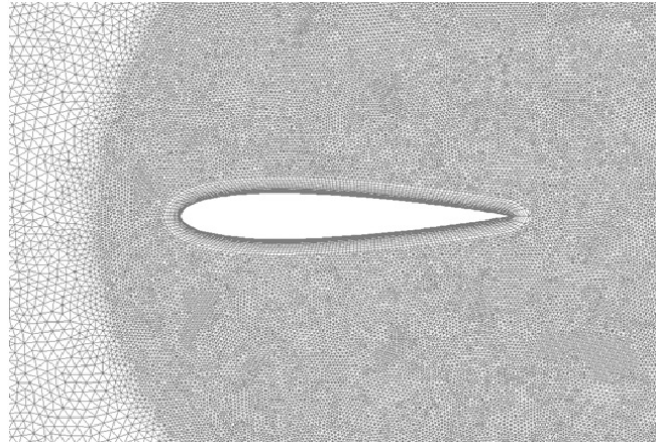


Figure 5.4: Zoomed view

energy equation was not turned on. The flow velocity supplied at the inlet was calculated from the chordal Reynolds number, as specified in the study that was validated. All solution quantities were solved using 2nd order discretization. The turbulence model used was K- SST[12,17], because it is highly effective in resolving boundary layer correctly.

5.3.4 Results

Figures 5.5-5.6 show the results of the validation study In figures 5.5-5.6 , the Case 1 depicts the results of our validation and Case 2 are the results of the study conducted by Liang C. et. Al. It can be clearly seen from the figures that an excellent agreement between the simulated and the validation results exist, and hence a valid computational model for further simulations has been established.

5.4 Simulations of the Optimised Airfoil

After a valid computational model has been set, we can now simulate the optimised airfoil, keeping all aspects of the model same[1,7,21]. This will allow us to compare the performance of the optimised airfoil with the baseline. Of course at this point this comparison would be of little use because we would only be comparing the lift drag characteristics. However, it will definitely give us insights into the performance and the relationship between the performance and the geometric characteristics of the airfoil. With that said, we can now begin with the simulations of the optimised airfoil.

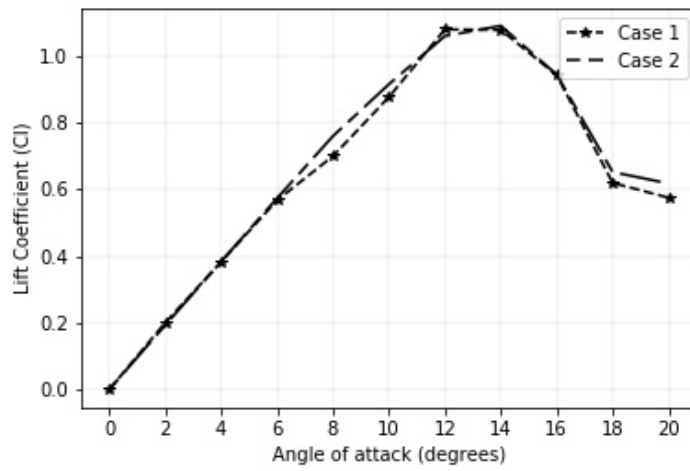


Figure 5.5: c_l vs α curves

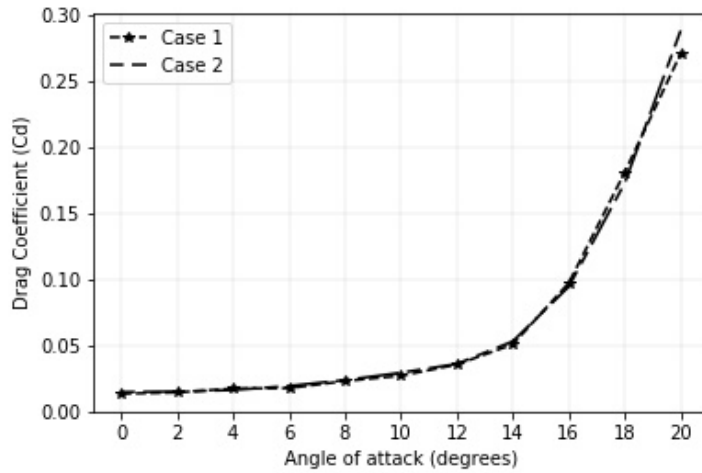


Figure 5.6: c_d vs α curves

5.4.1 Geometry Used

The geometry used in this case is the same as the one used in the previous case, the only difference being that the airfoil profile used is that of the optimised airfoil instead of the baseline. For the sake of brevity and not being repetitive the geometry has not been shown. However the reader can see the geometry in the subsequent meshing section.

5.4.2 Meshing

In this case the same meshing methods were retained so as not to change anything in the established computational method. Figure 5.7 shows the mesh used in this case, notice it looks almost identical to that used in the previous case.

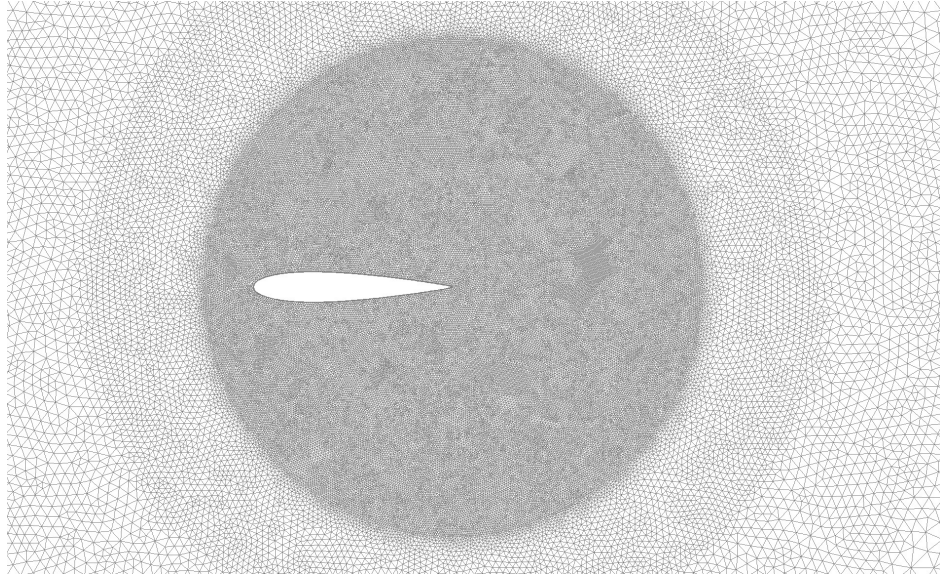


Figure 5.7: Mesh used for simulation

5.4.3 Setting the Solver

The same solver settings as in the previous case were used.

5.4.4 Results and Comparison

Figures 5.8-5.9 show the result of the comparison between the optimised and the baseline airfoil. It can be seen that the lift drag characteristics of the optimised airfoil are superior to the baseline airfoil. The tangential force coefficient, which is a measure of an airfoils suitability for application in a VAWT is superior in the case of the optimised airfoil. These improvements can be attributed to the fact that the airfoil possesses camber at the trailing edge which contributes significantly in the improving the Lift drag characteristics[9,13,17]. Furthermore the reduced thickness of the airfoil helps in decreasing separation, and allows the airfoil to be operated in low Reynolds number conditions[13,17]. Here it is important for the reader to understand that, even though this study more or less revolves around the low Reynolds

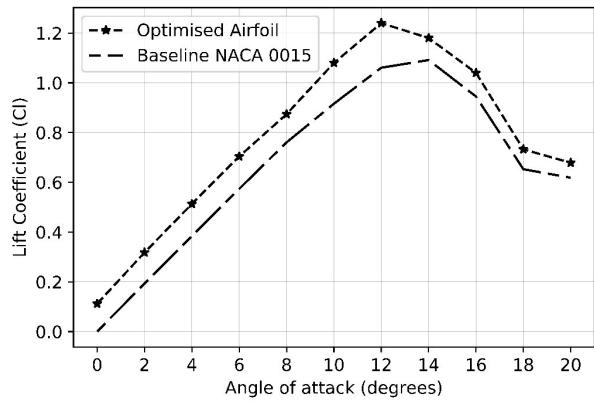


Figure 5.8: Comparing c_l vs α curves

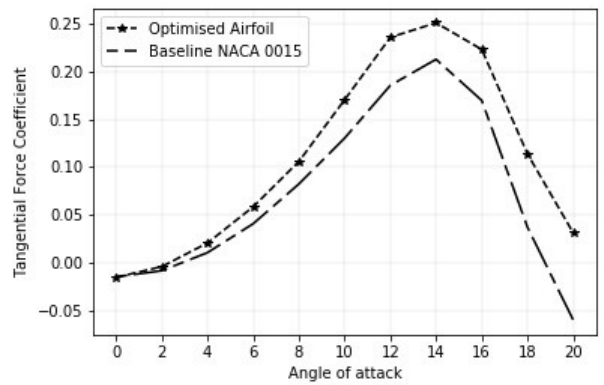


Figure 5.9: Comparing c_t vs α curves

number regime $8e4-7e5$, the comparison is made considering NACA 0015 as the baseline. There are two important reasons for this, firstly, this airfoil has been proven to possess good performance in VAWT applications[2,3,5,7,8,10]. Secondly, this study aims to provide an airfoil which has a better performance throughout the Re spectrum of VAWT operations. Which includes both very low Re (where a significant detachment and re-attachment occurs) and relatively high Re (Where the portion occupied by turbulent boundary layer is greater).

5.5 Mesh Independence Study

A mesh independence study was conducted to establish that the results obtained in the baseline airfoil optimisation are independent of the number of grid elements. Figure 5.10 shows the results of the grid independence study.

It can be seen that the mesh converges at approximately 160000 cells denoted by the red line in figure 5.10. This mesh independence study was done for the baseline airfoil validation. The results obtained were slightly different from the validation study, however the percentage difference in all cases was less than 9%, and so the results of this study were deemed acceptable.

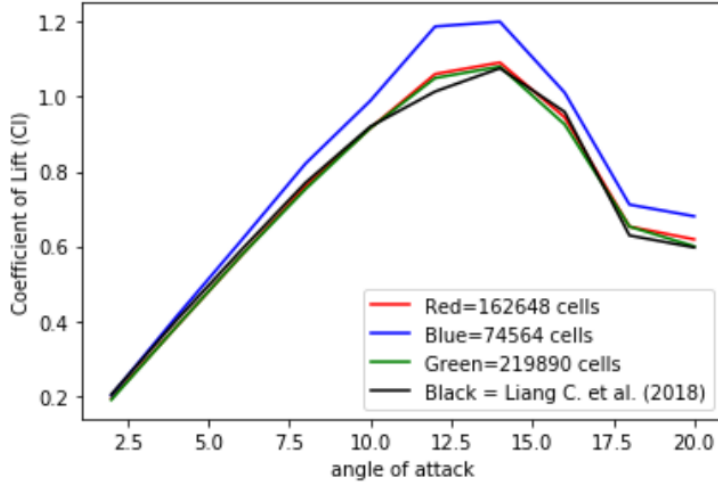


Figure 5.10: Grid Independence Study : C_l vs α curve

5.6 Simulations of VAWTs

Now that it has been established that the performance of the optimised airfoil is in fact better than the baseline performance, it becomes important to compare the two airfoils when they are parts of the VAWT. For this purpose simulations of VAWT in FLUENT were carried out. The process of simulation VAWTs is a comparatively long and tedious process. Before discussing the actual simulations, let us take a minute to understand the simulation procedure involved in simulating VAWTs. Firstly, it is important make a suitable geometry. Here the Sliding mesh methodology has been employed. This means that the transient behaviour of flow will induce vortices in the wake of the VAWT. These vortices have to be properly resolved in order to obtain an acceptable solution. The mesh therefore has to be finer (relatively) throughout. Furthermore, provisions for the rotation of the VAWT have to be made. For this, a sliding mesh methodology has been utilised. According to this methodology, the mesh rotates by some specific amount every timestep and the solver tries to solve for the flow every timestep in a domain that is ever so slightly changed (due to rotation). It then becomes important to set the timestep and other features properly.

5.6.1 Setting the Time-Step

It has been advised in the literature that, the time step should be chosen such that, one time step corresponds to 1 deg rotation of the VAWT. Therefore the time step calculation depends on the Angular

velocity(), and consequently on the tip-speed ratio. Table 5.2 shows the timestep set for different tip-speed ratios

TSR	ω (rad/s)	ω (rpm)	Δt_{1^o} (ms)
1	4	38.20	4.36
1.5	6	57.30	2.91
2	8	76.39	2.18
2.5	10	95.49	1.75
3	12	114.59	1.45
3.5	14	133.69	1.25
4	16	152.79	1.09

Table 5.2: Setting Time-steps

5.6.2 Setting Reference Values

In this section the reference values set in ansys fluent for the calculation of the moment coefficient (C_m) are shown. The reference values are extremely important. The magnitude of the moment coefficient is influenced by these values. Table 5.3 shows the reference values (general) that need to be set before beginning calculation

Parameter	Air (VAWT)
Density	1.225
Viscosity	1.7894e-5
Area	Turbine Diameter
Length	Turbine Radius
Velocity	As per Re_{chord}

Table 5.3: Reference Values

5.7 Validation Study of VAWT

The mesh and some of the models used for VAWT simulation are different from those chosen while simulating flow around airfoils. It is for this reason that a separate validation study needs to be conducted to setup a valid computational model for VAWTs[27]. This section contains details of the validation study conducted.

A. Setting up Geometry

In simulating VAWTs it is important that the domain used be sufficiently large, otherwise the physics of the flow is not captured. In these simulations a rectangular outer domain was used and a circular inner domain was used.

B. Mesh Used

The mesh was made sufficiently fine near the VAWT Blades and inflation layers were added to resolve the boundary layer better[27]. Mesh sizing was fixed to allow for the resolution of eddies in the wake of the VAWT[5,9,13,17]. Figures 5.11-5.12 show the mesh used in this simulation.

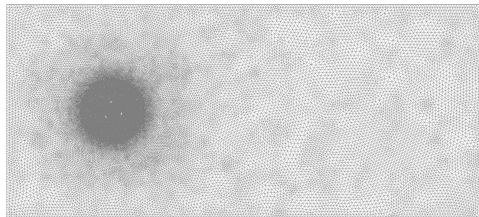


Figure 5.11: Mesh used for VAWT Simulation

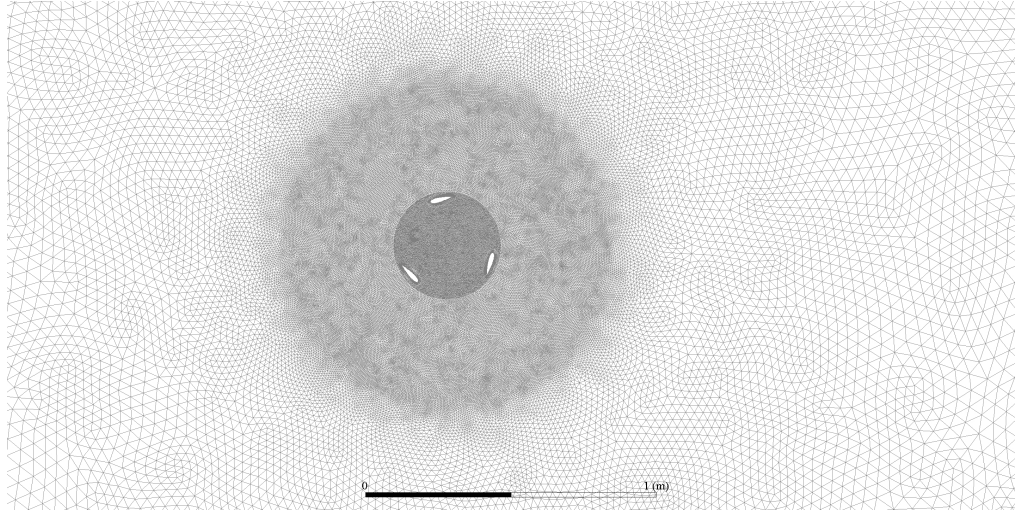


Figure 5.12: Zoomed view of mesh

In order to have a gradual size increase in this mesh, sphere of influence feature was used.

C. Named Selections

In the sliding mesh methodology, it is important to create mesh interfaces that allow the mesh to rotate and the flow to pass continuously across them, the mesh interfaces are created at the rotating boundary on both the sides of the mesh. Figure 5.13 shows the Named Selections used[27].

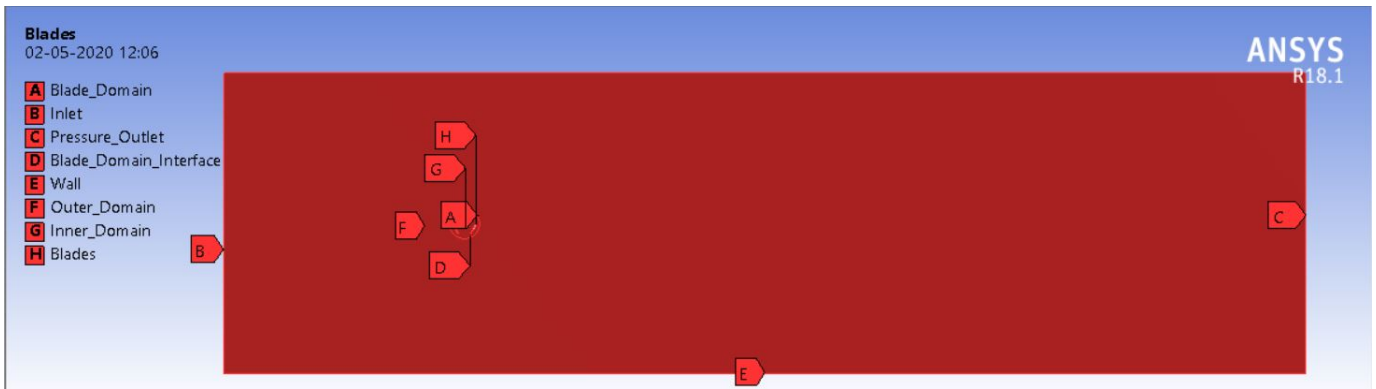


Figure 5.13: Named Selections for VAWT Study

D. Setting up the Solver settings

In this simulation a transient Pressure Based solver is used, transient solver is selected because of the sliding mesh methodology used. Furthermore, since the flow velocity was low, compressible effects were negligible, this allows for the use of a pressure based solver. The energy equation was turned off for this simulation. Turbulence was resolved using the k- SST turbulence model[12,17]. Production limiter

and Production Kato launder were used because a considerable amount of turbulence was expected in this simulation.

Furthermore in the solver settings, the under-relaxation factor for turbulent viscosity ratio was reduced from 1 to 0.75 to enhance solver stability.

E. Results

The criterion used for the comparison was the Coefficient of performance (C_p) vs tip-speed ratio (λ) curve. This curve was chosen because the C_p value take into account the lift and drag, hence a validation of the C_p more or less validates the lift and drag as well. Figure 5.14 shows the C_p vs λ for this simulation and the validation study[27]. It was found that an excellent agreement exists between the two curves. Here the published results refer to the study conducted by Brian H. Dennis et al. Figure 5.15(a) and (b)

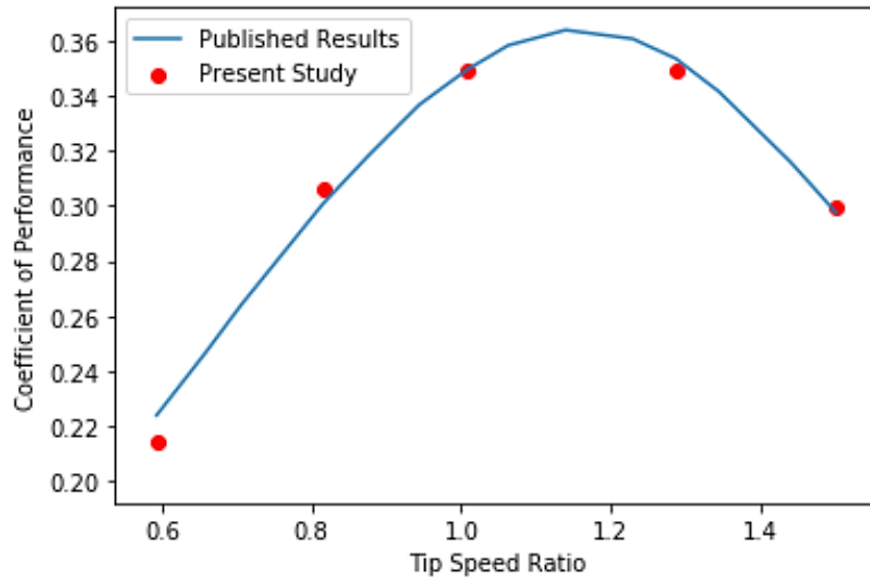


Figure 5.14: Comparing c_p vs λ curves for present study and validation study

shows the contours obtained from the simulations.

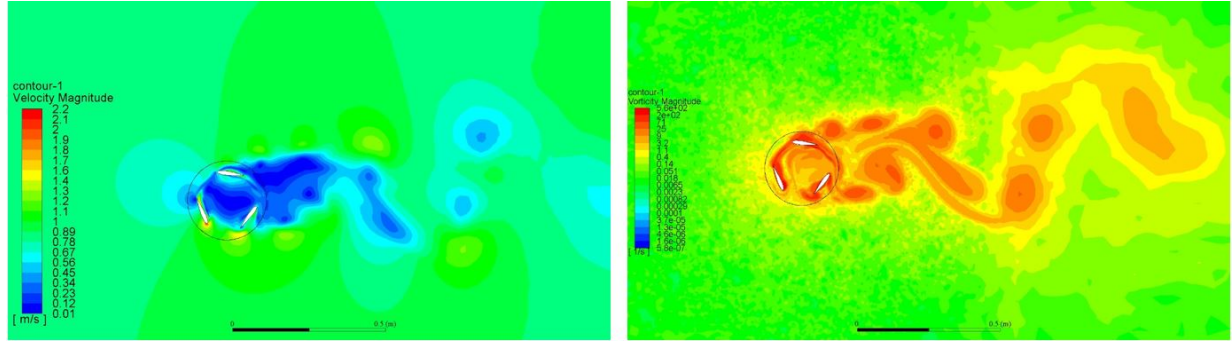


Figure 5.15: (a.) Velocity Magnitude (b.) Vorticity Magnitude

5.8 Discussion of the Nature of the Results

This section contains a brief discussion about the nature of the moment coefficient results obtained. This is particularly important to understand some basic principles pertinent to VAWTs. Figure 5.16 shows the plot of the instantaneous torque vs flow time. It can be seen that initially, the plot is non-periodic and ranges extreme values, this depicts the transient regime, wherein the numerical simulation marches towards a quasi-steady state. This means at this point the solution is moving towards a physically correct depiction of the flow from a pre-initialised depiction. This tells us about the dependence of the initialisation on the results. Better the initialisation, faster is the convergence. Furthermore, towards the end of the curve, a visible repeating pattern is visible. This depicts the quasi-steady/ periodic regime in the simulation. At this point the result has been obtained and further running the simulation just repeats the same pattern. Now, it is also important to understand that this pattern is highly dependent on the time-step size used. Smaller the time-step, more accurate is the solution but more time demanding it becomes. Hence it is important to find a trade-off between the accuracy and the amount of time required. This can be a separate study by itself, but is outside the scope of this one. Furthermore, an extremely small time-step ($1e-7$) does not guarantee a very precise result, other numerical errors like the round-off error and truncation error still exist[4,14,18].

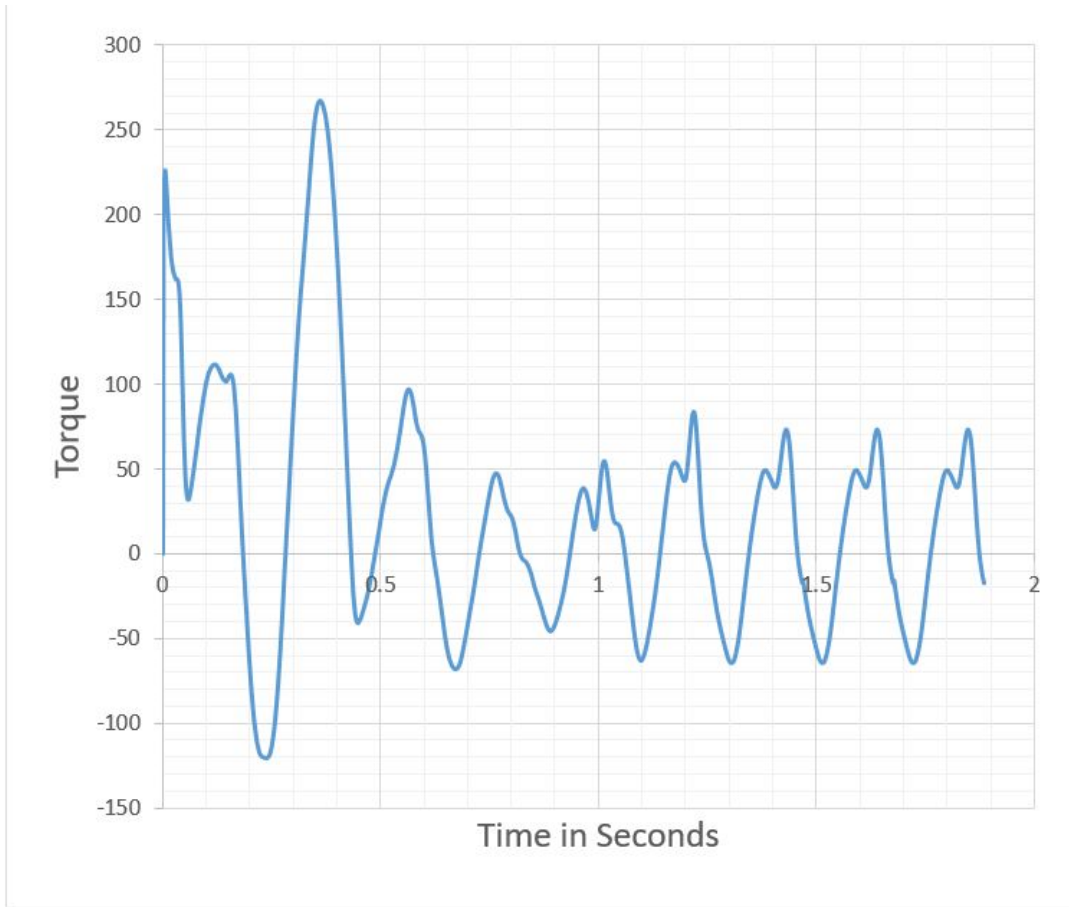


Figure 5.16: Discussion of the nature of the Results

5.9 Comparison Between Baseline VAWT and Optimised VAWT

This is the final section of this report and perhaps the most important part of it. In this section the results of a comparison between the optimised and the baseline airfoil are presented. It has been shown previously that the optimised airfoil performs better when the performance measurement is based on the lift-drag characteristics[1]. In this section the performance measurement shall be based on the coefficient of performance. The features of these simulations were the same as the validation study, this is so in order to retain the pre-validated case setups. The comparison was conducted for a $\lambda \in [1, 4.5]$ and a solidity of 0.2. This range is so chosen to match real-world results as much as possible. Figure 5.17 shows a comparison between the performance of the optimised airfoil and the baseline airfoil. Before beginning the simulations, it was expected that the performance of the optimised airfoil will be superior to the baseline at lower tip-speed ratios[1,2,6,7], as these also correspond to lower Reynolds numbers,

and then at higher Reynolds numbers, (i.e. high tip-speed ratios) the performance of the optimised airfoil would deteriorate, as it is thinner than the baseline. It appears that this pattern is followed in the simulations. Figure 5.17 shows the comparison of the C_p vs TSR for both the airfoils. It can be seen that the performance of the optimised airfoil is superior than the baseline at lower TSR values[3,5]. The performance then becomes almost identical to the baseline at lower TSR values. This happens because of the lower thickness of the optimised airfoil, which lends it a better performance at low TSR values, however it is this same feature that deteriorates the performance at high TSRs. The reason why the performance is not worse than the baseline is attributed to the camber that is introduced in this airfoil.

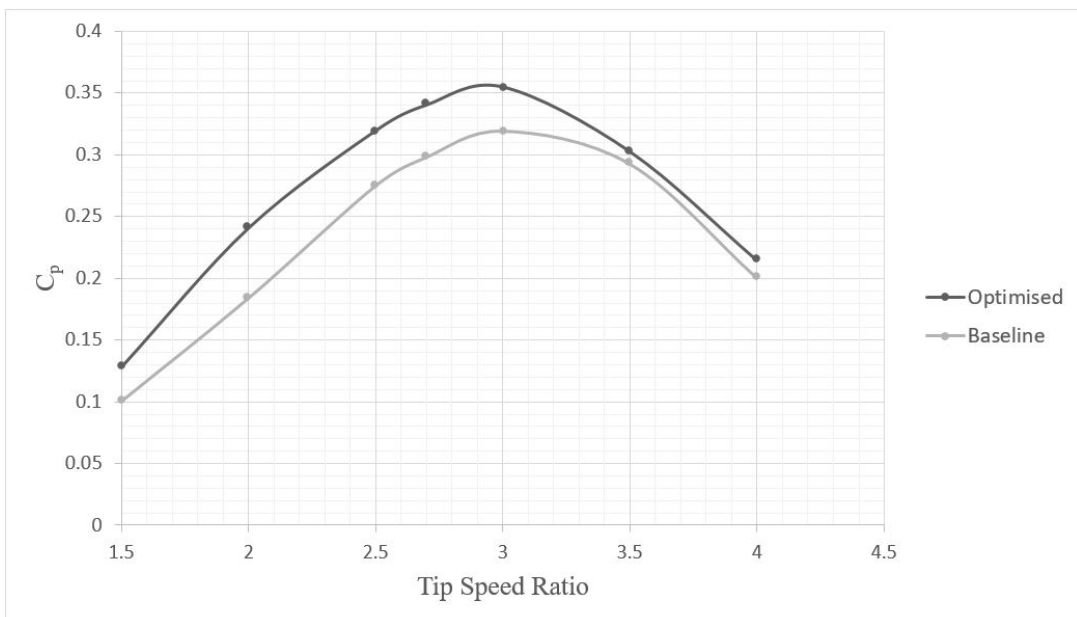


Figure 5.17: Comparing c_p vs λ curves for baseline and Optimised airfoil

5.10 Conclusion

In this report, a comparatively new and novel technique ha been explored to improve the performance of Vertical Axis Wind Turbines. This Heuristics based optimisation process has a lot of potential and can be developed further to produce even better candidate airfoils[10,14,15]. This report highlights the procedure of conduction an aerodynamic analysis of a VAWT in complete detail. This report also introduces the reader to the basics of Mathematical Optimisation and it's application to engineering design problems[26]. The results of this report are promising and indicate that optimisation techniques can produce more efficient designs of many engineering applications. The case considered here, Vertical Axis Wind Turbines can benefit a lot from mathematical optimisation techniques.

Coming swiftly to the specific results of this study, it was seen that

1. Gradient descent optimisation techniques are not well suited for airfoil optimisation[26].
2. Heuristic Based Optimisation Algorithms produced the best results although the time required by these algorithms is high. Genetic algorithms were used in this study, however other algorithms like particle swarm optimisation etc can be equally potent or perhaps even better for this problem. The reader is encouraged to use these algorithms.
3. High Camber airfoils are ill suited for application in VAWTs.[9,17,18,19]
4. Gurney flaps in high camber airfoils deteriorate their performance with regard to application in VAWTs[19,21].
5. Airfoils with reduced thickness are better suited for application in VAWTs designed for low λ values[17].
6. The performance of a thin airfoil can be increased for high λ values by introducing camber in them.
7. The ideal airfoil for use in Vertical axis wind turbines is one which provides almost equal performance in both, upside down state and upright state.

Further work on this Project

The use of different heuristics based optimisation techniques can be explored to compare the properties of convergence, the time taken to convergence and the quality of convergence. Furthermore the effect of addition of gurney flaps to lower camber and thin airfoils can be explored. Dynamic pitching for improved performance can be tried.

Bibliography

1. Badrya, C., Govindarajan, B., & Chopra, I. (2018). Basic Understanding of Unsteady Airfoil Aerodynamics at Low Reynolds Numbers. 2018 AIAA Aerospace Sciences Meeting. doi:10.2514/6.2018 – 2061
2. Battisti, L., Brighenti, A., Benini, E., & Castelli, M. R. (2016). Analysis of Different Blade Architectures on small VAWT Performance. Journal of Physics: Conference Series, 753, 062009. doi:10.1088/1742 – 6596/753/6/062009
3. Brownstein, I. D., Wei, N. J., & Dabiri, J. O. (2019). Aerodynamically Interacting Vertical-Axis Wind Turbines: Performance Enhancement and Three-Dimensional Flow. Energies, 12(14), 2724. doi:10.3390/en12142724
4. Castelli, M. R., Ardizzon, G., Battisti, L., Benini, E., & Pavesi, G. (2010). Modeling Strategy and Numerical Validation for a Darrieus Vertical Axis Micro-Wind Turbine. Volume 7: Fluid Flow, Heat Transfer and Thermal Systems, Parts A and B. doi:10.1115/imece2010 – 39548
5. Dumitrescu, H., Cardo, V., & Mlel, I. (2015). The Physics of Starting Process for Vertical Axis Wind Turbines. Springer Tracts in Mechanical Engineering CFD for Wind and Tidal Offshore Turbines, 6981. doi: 10.1007/978 – 3 – 319 – 16202 – 7
6. Gardner, B., & Selig, M. (2003). Airfoil Design Using a Genetic Algorithm and an Inverse Method. 41st Aerospace Sciences Meeting and Exhibit. doi:10.2514/6.2003 – 43

7. Hara, Y., Hara, K., & Hayashi, T. (2012). Moment of Inertia Dependence of Vertical Axis Wind Turbines in Pulsating Winds. International Journal of Rotating Machinery, 2012, 112. doi:10.1155/2012/910940
8. Kavade, R., & Ghanegaonkar, P. (2018). Effect of best position blade pitching on power coefficient of VAWT at different tip speed ratio by SST & DMST model. FME Transactions, 46(4), 560566. doi:10.5937/fmet1804560k
9. Li, S., Li, Y., Yang, C., Zhang, X., Wang, Q., Li, D., Wang, T. (2018). Design and Testing of a LUT Airfoil for Straight-Bladed Vertical Axis Wind Turbines. Applied Sciences, 8(11), 2266. doi:10.3390/app8112266
10. Liang, C., & Li, H. (2018). Aerofoil optimization for improving the power performance of a vertical axis wind turbine using multiple streamtube model and genetic algorithm. Royal Society Open Science, 5(7), 180540. doi: 10.1098/rsos.180540
11. Malan, P., Suluksna, K., & Juntasaro, E. (2009). Calibrating the $\gamma - Re_\theta$ Transition Model for Commercial CFD. 47th AIAA Aerospace Sciences Meeting Including The New Horizons Forum and Aerospace Exposition. doi:10.2514/6.2009 – 1142
12. Mauro, S., Lanzafame, R., Messina, M., & Pirrello, D. (2017). Transition turbulence model calibration for wind turbine airfoil characterization through the use of a Micro-Genetic Algorithm. International Journal of Energy and Environmental Engineering, 8(4), 359374. doi:10.1007/s40095 – 017 – 0248 – 2
13. Pendharkar, A., McGowan, R., Morillas, K., Pinder, M., & Komera, N. (2012). Optimization of a Vertical Axis Micro Wind Turbine for Low Tip Speed Ratio Operation. 10th International Energy Conversion Engineering Conference. doi:10.2514/6.2012 – 4244
14. Peng, H., Han, Z., Liu, H., Lin, K., & Lam, H. (2020). Assessment and optimization of the power performance of twin vertical axis wind turbines via numerical simulations. Renewable Energy, 147, 4354. doi: 10.1016/j.renene.2019.08.124

15. Qamar, S. B., & Janajreh, I. (2017). Investigation of Effect of Cambered Blades on Darrieus VAWTs. *Energy Procedia*, 105, 537543. doi:10.1016/j.egypro.2017.03.353
16. Rocchio, B., Deluca, S., Salvetti, M., & Zanforlin, S. (2018). Development of a BEM-CFD tool for Vertical Axis Wind Turbines based on the Actuator Disk Model. *Energy Procedia*, 148, 10101017. doi:10.1016/j.egypro.2018.08.060
17. Treatment of Low Reynolds Number Turbulence. (n.d.). *Modeling and Simulation of Turbulent Flows*, 347384. doi:10.1002/9780470610848.ch13
18. Zamani, M., Maghrebi, M. J., & Moshizi, S. A. (2016). Numerical study of airfoil thickness effects on the performance of J-shaped straight blade vertical axis wind turbine. *Wind and Structures*, 22(5), 595616. doi:10.12989/was.2016.22.5.595
19. Hao, L. and Gao, Y., 2019. Effect of Gurney Flap Geometry on a S809 Airfoil. *International Journal of Aerospace Engineering*, 2019, pp.1-8. doi:10.1155/2019/9875968
20. Jain, S., Sitaram, N. and Krishnaswamy, S., 2015. Computational Investigations on the Effects of Gurney Flap on Airfoil Aerodynamics. *International Scholarly Research Notices*, 2015, pp.1-11. doi:10.1155/2015/402358
21. Yan, Y., Avital, E., Williams, J. and Korakianitis, T., 2019. CFD Analysis for the Performance of Gurney Flap on Aerofoil and Vertical Axis Turbine. *International Journal of Mechanical Engineering and Robotics Research*, pp.385-392. doi:10.18178/ijmerr.8.3.
22. Li, Y., Wang, J. and Zhang, P., 2003. Influences of Mounting Angles and Locations on the Effects of Gurney Flaps. *Journal of Aircraft*, 40(3), pp.494-498. doi:10.2514/2.3144
23. Jin, X., Zhao, G., Gao, K. and Ju, W., 2015. Darrieus vertical axis wind turbine: Basic research methods. *Renewable and Sustainable Energy Reviews*, 42, pp.212-225. doi:10.1016/j.rser.2014.10.021
24. Castelli, M., Ardizzon, G., Battisti, L., Benini, E. and Pavesi, G., 2010. Modeling strategy and numerical validation for a darrieus vertical

- axis micro-wind turbine. International Mechanical Engineering Congress & Exposition IMECE2010, pp.1-11.
25. Aslam Bhutta, M., Hayat, N., Farooq, A., Ali, Z., Jamil, S. and Hussain, Z., 2012. Vertical axis wind turbine A review of various configurations and design techniques. Renewable and Sustainable Energy Reviews, 16(4), pp.1926-1939. doi:10.1016/j.rser.2011.12.004
26. Nature-Inspired Algorithms for Optimisation. (2009). Studies in Computational Intelligence. doi:10.1007/978 – 3 – 642 – 00267 – 0
27. Carrigan, T., Dennis, B., Han, Z., & Wang, B. (2014). Aerodynamic Shape Optimization of a Vertical-Axis Wind Turbine Using Differential Evolution. Wind Turbine Technology, 79121. doi:10.1201/b16587 – 6

Appendix : 1

This section contains the Pseudo code used for optimisation. This code explains the mechanism of implementing a genetic algorithm. This code can be extended to optimise any parameter in possibly any application. The pseudo code for geometry generation is not included, as the geometry generation can be done using many algorithms. For the generation of the geometry, Bezier curves and NURBS method had been used in this report. It was found that the NURBS method produced accurate airfoil geometries when compared to bezier curves. However the implementation of Bezier curves was found to be simpler.

Main File

```
from xfoil_program import the relevant functions
import relevant_packages
from airfoil_Generation_program import relevant functions

status = check if .dat or .log files exist in the current directory
is status == true
    delete all the files # Starting from a clean slate

initialise individuals_with_genes #attributes like thickness and camber are the genes

define upper_bound for the gene values
define lower_bound for the gene values

initialise variable for storing the indexing_airfoils

function restrict_genes_to_domain( input arg = present_individual)
```

```

check if any gene in present individual < lower_bound
    gene = lower_bound # limiting the gene value between allowed range
check if any gene in present individual > upper_bound
    gene = upper_bound # limiting the gene value between allowed range
end function

function breed_population_randomly
    initialise the population with n individuals
        initialisation to be done randomly using a uniform or normal distribution
end function

function generate_mutations_in_genes
    define a scale           # (percentage change)/2 of the gene magnitude
    genes = parent * ( 1 + random(-scale,scale))
    function call \textbf{restrict_genes_to_domain}
end function

function crossover_genes_from_parents
    define constant crossover point or define crossover randomly
    for all genes < crossover point
        offspring = parent_1
    else
        offspring = parent_2
    function call restrict_genes_to_domain
end function

define individuals per population
define Number of Generations
define Best_Individuals_to_output

-----
function Initialisation
    in a range of number_of_individuals
        population = breed_population_randomly

```

```

function call Generate airfoil profile from the genes in individual
function call Calculate the Fitness
save the results in a file
end function

function modify_present_generation
function call generate_mutations_in_genes
find_best = sort population based on fitness (reverse = true)
save best_3_individuals_from_population and pass them to next generation
take rest of the population and call function crossover_genes_from_parents
end function

function modify_the_best
best = sort population based on fitness (reverse = true)
take the best 7 individuals
function call generate_mutations_in_genes
function call crossover_genes_from_parents
blend the resulting airfoils in the population
end function

for i in range(0, iterations/generations)
call functions
-----
```

END OF PROGRAM